

DEVELOPMENT OF A FRACTIONAL LOOP ANTENNA IN FRONT OF A 60° CORNER REFLECTOR

A Thesis

Submitted to the Department of Electrical and Electronic Engineering, BUET, Dhaka in
partial fulfillment of the requirements for the degree

of

MASTER OF SCIENCE IN ELECTRICAL AND ELECTRONIC ENGINEERING



by

Md. Nur Mahabubul Alam Chowdhury

DEPARTMENT OF ELECTRICAL AND ELECTRONIC ENGINEERING
BANGLADESH UNIVERSITY OF ENGINEERING AND TECHNOLOGY

JUNE, 1997



CERTIFICATE

This is to certify that the work presented in this thesis was done by me under the complete supervision of Dr. Pran Kanai Saha, Associate Professor, Department of Electrical and Electronic Engineering, BUET, Dhaka, Bangladesh. It is also certified that this thesis work has not been submitted for the award of any degree or diploma.

Countersigned :



(Dr. Pran Kanai Saha)



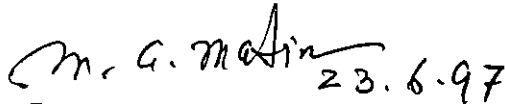
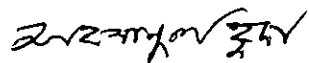


(Md. Nur Mahabubul Alam Chowdhury)

The thesis titled " **DEVELOPMENT OF A FRACTIONAL LOOP ANTENNA IN FRONT OF A 60° CORNER REFLECTOR** ", submitted by Md. Nur Mahabubul Alam Chowdhury, Roll No. 930643F, Registration No. 93730, Session : 1992-93-94 of M. Sc. in Engineering has been accepted as satisfactory in partial fulfillment of the requirements for the degree of

Master of Science in Electrical and Electronic Engineering.

Board of Examiners

1.  23/6/97
DR. PRAN KANAI SAHA
Associate Professor
Department of Electrical & Electronic Engineering
BUET, Dhaka - 1000. Chairman
(Supervisor)
2. 
DR. MD. QUAMRUL AHSAN
Professor & Head
Department of Electrical & Electronic Engineering
BUET, Dhaka - 1000. Member
(Ex-Officio)
3.  23.6.97
DR. MD. ABDUL MATIN
Professor
Department of Electrical & Electronic Engineering
BUET, Dhaka - 1000. Member
4.  23/6/1997
AHSANUL HUDA
Professor & Head
Department of Electrical & Electronic Engineering
BIT Dhaka, Gazipur - 1700. Member
(External)

ACKNOWLEDGMENT

The author would like to express his deepest gratitude to his advisor, Dr. Pran Kanai Saha who patiently gave many invaluable advises, continuous guidance, and constant encouragement during thesis work.

Special thanks to Prof. Dr. Abdul Matin and Prof. Ahsanul Huda for their cooperation in getting the experimental results and the necessary information about the research.

The author takes this opportunity to express his deepest appreciation to Dr. Md. Quamrul Ahsan, Professor and Head of the Department of Electrical and Electronic Engineering, BUET for providing departmental facilities.

Grateful acknowledgment is also made for the research grants provided by the authority of BUET that allowed the author to conduct the research.

Finally, author would like to give thanks to them who directly or indirectly helped in this research work, specially, to Md. Nurunnobi Mollah, Assistant Professor, Electrical and Electronic Engineering Department, BIT Khulna for his encouragement to do this research.

ABSTRACT

The level of shielding of the enclosure in preventing EMI is usually determined through the Shielding Effectiveness (SE) measurements of the material used for the enclosure. Standard field simulation is the starting point of any SE measurement technique. Thus it is necessary for an antenna which could simulate standard EM waves.

In this research work a Hexad-Loop (H-Loop) antenna has been proposed to simulate standard EM wave for magnetic-field shielding effectiveness measurement of the planar sheet. In making the H-loop antenna one sixth of a loop is mounted on a 60° corner reflector to produce the effect of magnetic dipole in a confined region. The imaging effect of the reflector transforms the H-loop virtually into a complete loop which means the H-loop acts as a magnetic dipole in front of the reflector with negligible radiation behind the reflector. Thus it produces typical low impedance field in a quasi-shielded test environment which is particularly important in the measurement of magnetic field SE against EMI.

The mathematical model of the H-loop antenna has been developed by using the image theory and the theory of pattern multiplication. Analytically, the field due to the arc (one sixth of the loop) is to be calculated first and then applying image theory for determining the images of the arc. The effect of these images on the field of the original H-loop are then superimposed by a method similar to pattern multiplication.

The radiation patterns of the H-Loop antenna in the horizontal plane is measured by using the two H-Loop antenna (one acts as a transmitting antenna while the other acts as a receiving antenna). Measured radiation pattern is found identical with the theoretical pattern.

The antenna parameters such as, directivity, gain, and radiation efficiency of the H-Loop antenna are compared with those of the Q-Loop and complete loop antenna. Comparison shows that, both the directivity and gain of the H-Loop antenna are much higher than those of the existing antenna. It is also found that the gain and radiation efficiency of the H-Loop antenna become constant at frequency above 100MHz. This means that the developed antenna can be treated as a frequency independent antenna above 100MHz.

The radiation resistance, loop and reflector resistance, loop inductance, and the capacitance of the H-Loop are determined analytically.

CONTENTS

	Pages
Certificate	ii
Board of Examiners	iii
Acknowledgment	iv
Abstract	v
List of Acronyms	xi
List of Symbols	xii
List of Figures	xiv
List of Tables	xvii

CHAPTER 1 GENERAL INTRODUCTION

1.0	Introduction	1
1.1	Important Features of EMC Antennas	2
	1.1.1 Frequency of operation	2
	1.1.2 Directional property and Gain	3
	1.1.3 Standard field simulation	3
	1.1.4 Shielding performance against ambient noise	3
1.2	Review	4
1.3	Aim and Objectives of the Thesis	5
1.4	Organization of the Thesis	6

CHAPTER 2 THEORETICAL BACKGROUND

2.0	Introduction	7
2.1	Characteristics of Near Magnetic Field Source	7
2.2	H-Loop Antenna as Near Magnetic Field Source	10
2.2.1	Principle of pattern multiplication	11
2.2.2	Images of a one sixth of loop in front of a corner reflector	11
2.3	Antenna Parameters	13
2.3.1	Directivity	13
2.3.2	Gain	15
2.3.3	Radiation pattern	16

CHAPTER 3 MATHEMATICAL MODEL AND COMPARISON

3.0	Introduction	17
3.1	Mathematical Model of H-Loop Antenna	17
3.1.1	Distances between dipoles and observation points	18
3.1.2	Vector potential of coplanar hexad dipoles	22
3.1.3	Vector potential of the H-Loop element	24
3.1.4	Field computation	26
3.2	H-Loop Antenna Parameters	28
3.2.1	Directivity	29
3.2.2	Radiation resistance	30
3.2.3	Loop and Reflector resistance	31
3.2.4	Inductance of the H-Loop	32

3.2.5	Capacitance of the H-Loop	34
3.2.6	Gain	36
3.3	Comparison	37
3.3.1	Comparison of field component with the Q-Loop antenna and complete loop antenna	38
3.3.2	Antenna parameters	39

CHAPTER 4 DESIGN, CONSTRUCTION AND ANTENNA MEASUREMENT

4.0	Introduction	41
4.1	Design Construction of Fractional Loop	41
4.1.1	Loop Radius	41
4.1.2	Shape and Dimension of the loop cross section	43
4.2	Construction of Hexad of a Loop	44
4.3	Design consideration of the Reflector	45
4.4	Construction of the Reflector	46
4.5	Construction of the H-Loop Antenna	47
4.6	Field Measurement	49
4.6.1	Test set-up	50
4.6.2	Instrument and other Accessories for field measurement	51
4.6.2.1	Unit Oscillator	52
4.6.2.2	I.F. Amplifier and Mixer rectifier	52
4.6.3	Feed arrangement	53
4.6.4	Measurement procedure	54
4.6.5	Test results and Comparison	55

4.7	Computation and Comparison of Antenna Parameters	59
4.7.1	Directivity	60
4.7.2	Gain	60
4.7.3	Radiation efficiency	62
4.7.4	Radiation resistance	63

CHAPTER 5 CONCLUSION AND RECOMMENDATIONS FOR FUTURE WORK

5.1	Conclusion	65
5.2	Recommendations for Future Work	67

APPENDICES

Appendix A	Output Power Level of a Unit Oscillator at various Frequencies	68
Appendix B	Relation between the Amplitude of the Radiated Field and the Amplitude of the Input Signal of the I.F. Amplifier	69

REFERENCES	72
-------------------	-----------

LIST OF ACRONYMS

EMC	Electromagnetic Compatibility
EMI	Electromagnetic Interference
SE	Shielding Effectiveness
IL	Insertion Loss
MUT	Material Under Test
TEM	Transverse Electromagnetic
TE	Transverse Electric
RF	Radio Frequency
OATS	Open Area Test Site
Q-Loop	Quarter of a Loop
H-Loop	Hexad of a loop

LIST OF SYMBOLS

c	speed of light ($= 3 \times 10^8$ m/s)
f	frequency, Hz
α	angle between the reflector sheet
β	phase constant ($= 2\pi/\lambda$, rad/m)
ϵ	permittivity, F/m
ϵ_0	permittivity of free space ($= 8.852 \times 10^{-12}$ F/m)
μ	permeability, H/m
μ_0	permeability of free space ($= 4\pi \times 10^{-7}$ H/M)
ϕ	azimuth angle, rad
θ	polar angle, rad
λ	wave length, m
λ_0	wave length in free space, m
σ	conductivity ($= 5.7 \times 10^7$ mho/m)
ω	angular frequency ($= 2\pi f$, rad/sec)
\Re	real part
\vec{A}	vector magnetic potential
\vec{E}	electric field vector, V/m
\vec{H}	magnetic field vector, A/m
\hat{x}	unit vector along the x direction
\hat{y}	unit vector along the y direction
$\hat{\phi}$	unit vector along the ϕ direction

D	directivity
U_{av}	average radiation intensity
U_m	maximum radiation intensity
P_r	radiated power, watts
S_r	poynting vector, W/m²
G	gain, dB
η	radiation efficiency
Z_o	intrinsic impedance (= 377Ω in free space)

LIST OF FIGURES

	Pages
Figure : 2.1(a) Radiated field in the far region of a loop antenna.	9
Figure : 2.1(b) Wave impedance depends on the distance from the source and on whether the field is electric or magnetic.	9
Figure : 2.2 A 60° corner reflector with images.	10
Figure : 2.3 Image produces by an infinitesimal dipole of one sixth of loop in front of a 60° corner reflector.	12
Figure : 3.1 Array of coplanar three pairs of dipole.	18
Figure : 3.2 Far field of three pairs of dipoles, arbitrarily oriented w.r.t. the axes of co-ordinates.	19
Figure : 3.3 Geometry of one sixth of loop for determining the vector potential of the H-Loop arc.	19
Figure : 3.4(a) Planar radiation pattern (E_ϕ) of the H-Loop antenna on $\phi = 30^\circ$ plane with θ varying from 0 to 360° .	28
Figure : 3.4(b) Planar radiation pattern (E_ϕ) of the H-Loop antenna on $\theta = 90^\circ$ plane with ϕ varying from 0 to 360° .	28
Figure : 3.5 Model of stray capacitance of the H-Loop antenna.	35

Figure : 4.1(a)	Gain vs Frequency curve at various loop radius.	42
Figure : 4.1(b)	Radiation efficiency vs Frequency curve at various loop radius.	42
Figure : 4.2	Radiation efficiency vs Frequency curve at various wire radius.	43
Figure : 4.3(a)	Sectional view of a hexad loop.	44
Figure : 4.3(b)	Dimensions and screw positions of the hexad loop.	45
Figure : 4.4	Design of a 60° corner reflector.	46
Figure : 4.5	Detailed diagram of H-Loop antenna.	47
Figure : 4.6(a)	Photograph of front view of the H-Loop antenna.	48
Figure : 4.6(b)	Photograph of top view of the H-loop antenna.	48
Figure : 4.7	Field pattern measurement set-up.	50
Figure : 4.8	Photograph of field pattern measurement set-up.	51
Figure : 4.9	Block diagram of Type 874 -MR mixer rectifier.	53
Figure : 4.10	Photograph of rear end of the H-Loop antenna.	54
Figure : 4.11	Radiated field pattern at $\theta = 90^\circ$ and ϕ varying from 0 to 180° at a radial distance of 1m (a) 150MHz; (b) 200MHz; and (c) 250MHz.	56
Figure : 4.12	Radiated field pattern at $\theta = 90^\circ$ and ϕ varying from 0 to 180° at a radial distance of 2m (a) 150MHz; (b) 200MHz; and (c) 250MHz.	57
Figure : 4.13	Radiated field pattern at $\theta = 90^\circ$ and ϕ varying from 0 to 180° at a radial distance of 3m (a) 150MHz; (b) 200MHz; and (c) 250MHz.	58
Figure : 4.14	Theoretical radiated field pattern of the H-loop antenna at $\theta = 90^\circ$ and ϕ varying from 0 to 180° .	59

Figure : 4.15	Gain vs Frequency curve at a loop radius of 15cm.	61
Figure : 4.16	Comparison of Gain.	61
Figure : 4.17	Radiation efficiency vs Frequency curve at a given loop radius of 15cm.	62
Figure : 4.18	Comparison of Radiation efficiency.	63
Figure : 4.19	Radiation resistance vs Frequency curve at a given loop radius of 15cm.	64
Figure : A1	Output power level of a typical type 1208-C unit oscillator into a 50 Ω coaxial load.	68
Figure : B1	Block diagram of the receiving section of field pattern measurement set-up.	69

LIST OF TABLES

	Pages
Table - 1 : Comparison of Directivity.	39
Table - 2 : Comparison of Gain.	40

CHAPTER 1



GENERAL INTRODUCTION

- INTRODUCTION
- IMPORTANT FEATURES OF EMC ANTENNAS
- REVIEW
- AIM AND OBJECTIVES OF THE THESIS
- ORGANIZATION OF THE THESIS

1.0 INTRODUCTION

Scientists and engineers in the field of Electromagnetic Compatibility (EMC) are always interested in designing electronic systems which are invulnerable to hostile or interfering electromagnetic environment and at the same time electromagnetically harmless to their neighbouring devices. The simplest way of reducing ingress or emission of Electromagnetic Interference (EMI) is by enclosing electrical and electronic equipment using conducting materials. Again, the level of shielding of the enclosure against EMI is usually determined by the measurement of Shielding Effectiveness (SE) of the material used for the enclosure [1].

The term shield usually refers to a metallic enclosure that completely encloses an electronic product or a portion of that product. Enclosure can prevent the propagation of electric and magnetic fields from the product to the outside and from outside to the product, which may cause EMI in the product.

Therefore, the effectiveness of a shield refer to shielding effectiveness (SE), is an important factor to protect EMI in the product. SE is defined as the ratio of the magnitude of the electric (magnetic) field that is incident on the shield to the magnitude of the electric (magnetic) field that is transmitted through the shield. Thus, during SE measurement it is usual practice to measure the insertion loss (IL). IL is measured by comparing the received signal strength with and without the material under test (MUT) in the test device [2].

The standard field simulation is the starting point of any SE measurement technique. Hence it is necessary for an antenna as a EM source which could produced standard EM waves.

On the basis of the distance (r) between EM source and the MUT, SE measurement can be classified [2] as (i) Far field SE measurement (distance $r > 0.166\lambda$, where λ is the wavelength) and (ii) Near field SE measurement ($r < 0.166\lambda$). Near field SE measurement

can again be classified as Near electric-field SE measurement where source is predominantly electric field and Near magnetic-field SE measurement where source is predominantly magnetic field. This research work aims at developing an antenna which could simulate predominantly magnetic field in the near field region.

In this thesis a newly developed Hexad-loop (H-loop) antenna has been proposed for magnetic field shielding effectiveness measurement of the planar sheet. This loop acts as a complementary source to develop a predominantly magnetic field at the test location.

In designing the antenna, the factors which are to be considered are (i) range of frequency, (ii) directional property and gain, (iii) standard field simulation, and (iv) shielding performance. These factors have been described in section 1.1.

A comprehensive review of Near field SE measurement techniques is given in section 1.2. The aim and objectives of this thesis are presented in section 1.3. Section 1.4 contains the organization of this thesis.

1.1 IMPORTANT FEATURES OF EMC ANTENNAS

1.1.1 Frequency of operation (EMC range of frequency)

It is always desirable that an EMC antenna covers the frequency range of interest for EMC measurement. The typical frequency range for EMC measurement varies from 20MHz to 1GHz [3]. Thus in designing an EMC antenna, this frequency range is to be considered.

1.1.2 Directional property and Gain

One of the most important features of EMC antenna is its directional property. EMC measurement is generally performed in a shielded room which provides a high degree of isolation from EM environments. But multiple reflections from the room walls causes a significant measurement error. This error can be reduced if the measurement is done in an anechoic chamber which is very expensive because of absorbing materials. This cost can be reduced if a highly directive antenna (i.e. an antenna in front of a reflector) is used for EMC measurement in a shielded room. Because, only a small portion of the room walls are then needed to cover by the absorbing material.

Directivity of the antenna determines the directional property of the antenna. An antenna with high directivity can produce a stronger EM field on a specific test location in comparison with an antenna which may be a efficient radiator of having lower directivity. For constant efficiency, antenna gain will be increased with the increase of directivity.

1.1.3 Standard field simulation

Susceptibility measurements require the simulation of uniform plane wave whereas emission measurements require the simulation of either high impedance field or low impedance field at the test location. Thus one of the requirements for designing EMC antennas is the capability of producing the standard field at the test site. In this thesis work, the proposed EMC antenna can simulate low impedance field (i.e. magnetic field) at the test location.

1.1.4 Shielding performance against ambient noise

An EMC antenna is to be immune from background noise for ensuring the EM field produced by it.

1.2 REVIEW

Various methods for the measurement of magnetic field SE, which are being used by reputed EMC compliance testing organization for testing the shielding capability of shielded materials (in sheet form) are described below.

In MIL-STD 285 test method [4] transmitting antenna is placed in the shielded room whereas the receiving antenna is placed outside the room. The MUT sheet is mounted over an aperture in the wall of the shielded room. By comparing the transmission loss between the same two antennas with or without the MUT sheet, SE is measured according to IL equation described in the literature [2].

In the test arrangement of ASTM E57-83 [5], two chambers of small boxes pivoted at one end and the other end is clamped. The transmitting and receiving antennas are mounted inside the chamber to emit (or receive) the radiated power and the sample sheet is placed in between the walls of the two chambers. The data for SE measurement are taken as same as MIL-STD 285 test method.

A new method for the magnetic field SE measurement is reported by Rahman [6]. In this method the MUT is placed between the two Q-Loop (quarter loop) antenna. One is used as a transmitting antenna while the other is used as a receiving antenna. SE of the MUT sheet are then determined in a similar way to the MIL-STD 285 test method.

Hexad-Loop (H-Loop) of highly directive and high gain is proposed for magnetic field SE measurement.

The H-Loop antenna is used for near magnetic field source simulation. One sixth of a loop is mounted on a 60° corner reflector to produce the effect of magnetic dipole in a confined

region. The imaging effect of the reflector transforms the H-Loop virtually into a complete loop which means the H-Loop acts as a magnetic dipole in front of the reflector with negligible radiation behind the reflector. Thus it produces typical low impedance field in a quasi-shielded test environment which is particularly important in the measurement of magnetic field SE against EMI.

Two Hexad-Loop (H-Loop) antenna (one acts as a transmitting antenna while the other as a receiving antenna) can be used to measure the magnetic field SE of planar sheet like conductive material.

1.3 AIM AND OBJECTIVES OF THE THESIS

This research work is aimed at developing a fractional loop antenna in front of a 60° corner reflector. To fulfil the aim the following objectives were envisaged:

- Development of mathematical model of the H-Loop antenna by using image theory and the theory of pattern multiplication.
- Design and construction of the fractional loop.
- Design and construction of the reflector.
- Computation of the antenna parameters such as field patterns, directivity, gain, and radiation efficiency.
- Comparison of the developed antenna parameters with those of the Q-Loop and the

complete loop antenna.

-- Experimental validation of the far field pattern of the developed antenna.

1.4 ORGANIZATION OF THE THESIS

Theoretical background of the antenna theory is given in chapter 2. Magnetic field source simulation at the test location for the magnetic field SE measurement is also described in this chapter. Chapter 3 contains the mathematical model of H-Loop antenna. Comparison of the developed antenna parameters with those of the existing Q-Loop and the complete loop antenna is also given in this chapter. Design and construction of the H-Loop antenna are described in chapter 4. Measurement of field pattern of the developed antenna is also included in this chapter. Chapter 5 contains the conclusion and recommendations for further research.

CHAPTER 2

THEORETICAL BACKGROUND

- ❑ INTRODUCTION
- ❑ CHARACTERISTICS OF NEAR MAGNETIC FIELD SOURCE
- ❑ H-LOOP ANTENNA AS NEAR MAGNETIC FIELD SOURCE
- ❑ ANTENNA PARAMETERS

2.0 INTRODUCTION

An antenna which produces predominantly magnetic field is necessary for near magnetic field SE measurement. Thus the characteristics of near magnetic field source are described in section 2.1. It has already been stated in the previous chapter that Q-Loop and complete loop antenna produces predominantly magnetic field at the test location. In this research, a new antenna which can produce such field at the test location has been proposed. Section 2.2 describes the use of H-Loop antenna as a near magnetic field source. In the previous chapter it has already been mentioned various antenna parameters which indicate the performance of antenna. General equations to find the antenna parameters are given in section 2.3.

2.1 CHARACTERISTICS OF NEAR MAGNETIC-FIELD SOURCE

The radiated field available in the near-field region of a small loop antenna is the low impedance field. This can be explained by considering a circular loop of radius a with a uniform in phase current $I_0 e^{j\omega t}$. For very small loop radius (i.e. $a \leq \lambda/10$), the field radiated by the loop can be expressed as [7]:

$$E_r = E_\theta = H_\phi = 0 \quad (2.1)$$

$$H_r = \frac{\pi a^2 I_0 e^{j(\omega t - \beta r)} \cos\theta}{2\pi r} \left[\frac{j\beta}{r} + \frac{1}{r^2} \right] \quad (2.2)$$

$$H_\theta = -\frac{\pi a^2 I_0 e^{j(\omega t - \beta r)} \sin\theta}{4\pi r} \left[\beta^2 - \frac{j\beta}{r} - \frac{1}{r^2} \right] \quad (2.3)$$

$$E_{\phi} = -\frac{j\omega\mu_0\pi a^2 I_0 e^{j(\omega t - \beta r)} \sin\theta}{4\pi r} \left[j\beta + \frac{1}{r} \right] \quad (2.4)$$

It is evident from the above equation that at a large distance (i.e. $r \gg \lambda$), terms containing $1/r^2$ and $1/r^3$ may be neglected compared to the term containing $1/r$. The eqns. 2.1 to 2.4 then becomes as:

$$E_r = E_{\theta} = H_{\phi} = H_r = 0 \quad (2.5)$$

$$H_{\theta} = -\frac{\beta^2 a^2 I_0 e^{j(\omega t - \beta r)} \sin\theta}{4r} \quad (2.6)$$

$$E_{\phi} = -\frac{\beta\omega\mu_0 a^2 I_0 e^{j(\omega t - \beta r)} \sin\theta}{4r} \quad (2.7)$$

Thus in the far field region the radiated field of a loop antenna is Transverse Electromagnetic (TEM) in nature because of containing only the H_{θ} and E_{ϕ} component of the field. On the other hand eqns. 2.1 to 2.4 show that the $1/r^2$ and $1/r^3$ terms dominate over the $1/r$ terms (i.e. in the near field region). Thus in the near field region radial (H_r) and polar (H_{θ}) components of the magnetic field, and the azimuth component (E_{ϕ}) of the electric field are found. This means that the wave appears in the near field region is Transverse Electric (TE) in nature. The field radiated by a loop antenna and the wave impedance of this field is shown in fig. 2.1(a) and 2.1(b) respectively.

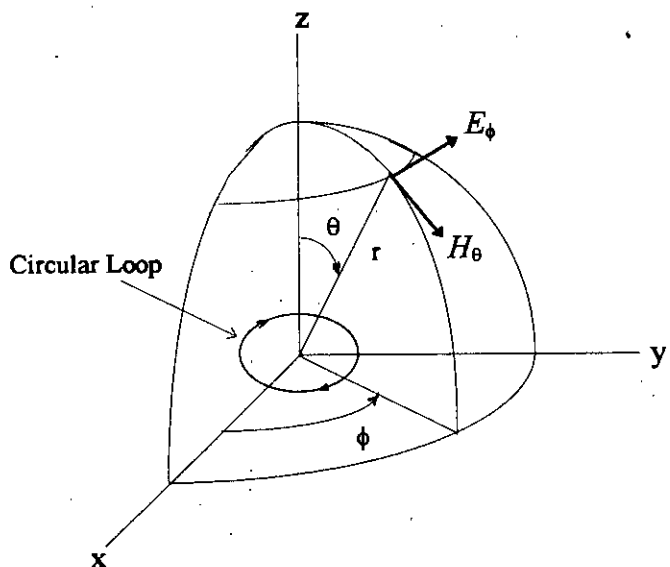


Fig. 2.1 (a) Radiated field in the far region of a loop antenna [8].

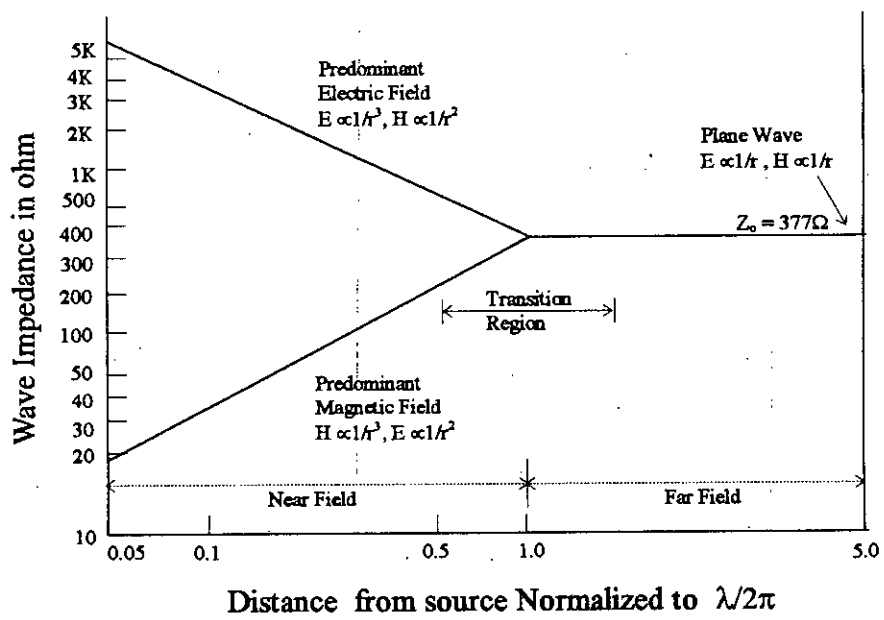


Fig. 2.1(b) Wave impedance depends on the distance from the source and on whether the field is electric or magnetic [2].

2.2 H-LOOP ANTENNA AS NEAR MAGNETIC-FIELD SOURCE

Reflectors are widely used to modify the radiation pattern of a radiating element such as antenna. It can improve the directional property of an antenna and can also yield a substantial gain in the forward radiation. A large flat metallic sheet reflector can convert a bi-directional antenna array into a unidirectional antenna array by eliminating the backward radiation from the antenna. With two such flat sheets intersecting at an angle α ($<180^\circ$), a sharper radiation pattern than that from a flat sheet reflector ($\alpha = 180^\circ$) can be achieved. This arrangement is known as active corner reflector antenna [8]. Thus, one sixth of a loop is placed in front of a 60° corner reflector to design the proposed loop antenna which can be used as a near magnetic field source.

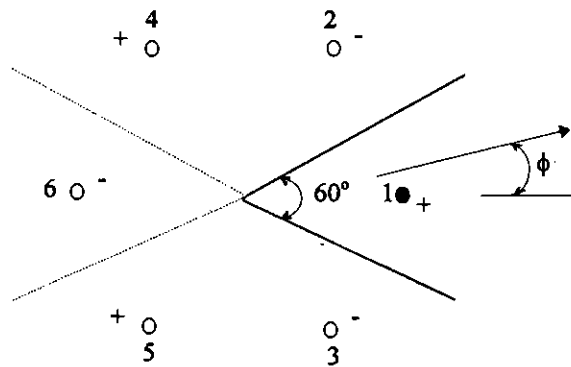


Fig. 2.2 A 60° corner reflector with images.

One sixth of a loop, placed in front of a 60° corner reflector produces another five images of one sixth of loop around the back side of the reflector which is equivalent to a complete loop in free space. This can be explained by the image theory and the theory of pattern multiplication. These two theories are described in the following subsections.

2.2.1 Principle of pattern multiplication

The principle of pattern multiplication can be stated as, "The field pattern of an array of nonisotropic but similar point sources is the product of the pattern of the individual source and the pattern of an array of isotropic point sources, having the same locations, related amplitudes and phases as the nonisotropic point sources" [8].

This principle has been employed to determine the field pattern of the proposed H-Loop antenna. To do so, the field due to the arc (i.e. one sixth of the loop) is calculated first and then the images of the arc are determined by applying image theory. The effect of these images on the field of the original loop are then superimposed by a method similar to pattern multiplication as described in the previous paragraph.

2.2.2 Images of a one sixth of loop in front of a corner reflector

The image produced by the one sixth of loop in front of a corner reflector can be studied by using the principle of reflection and the image theory [8]. The principle of reflection states that when a direct wave is reflected from the perfect conducting ground, the tangential component of the electric field must vanish at its surface. To fulfill this boundary condition, the reflected wave must suffer a phase of 180° at the point of reflection. Thus due to the presence of this perfect ground, the field at a distant point is the resultant of a direct wave and a reflected wave. This method is known as the method of images. According to the image theory an ideal dipole oriented normal to a perfect conducting infinite ground plane produces an image dipole equidistant from the ground plane. The image dipole is also oriented normal to the ground plane and carries the same current as that of the original one whereas the dipole oriented parallel to the ground plane produces the image dipole which is also oriented in parallel to the ground plane. The parallel image dipole carries a current which

is equal in magnitude but opposite in direction to that of the original one. It is well accepted that instead of the infinite ground plane the image theory is also applicable if the conducting ground plane extends beyond the dipole by several times of the length of the dipole which is very close to the conducting plane.

The reflection behavior of a 60° corner reflector of the proposed antenna can be explained by employing the image theory. A parallelly oriented dipole in front of a 60° corner reflector, produces five images to satisfy the boundary condition as mentioned in the previous paragraph. The image theory can be extended for the analysis of a one sixth of loop which is composed of infinitesimal dipoles of length $ad\phi$ (such as the dipole at A_1 shown in fig. 2.3), oriented normal to the reflector. Image theory straightway refers to the two images at A_2 and A_3 because of the reflectors OR_1 and OR_2 . If we take the corner line as a reflector then the third image A_6 is to be considered. Again, another two images A_4 and A_5 images are produced due to the image reflector OR_4 and OR_3 respectively. Therefore, each infinitesimal dipole element of the arc would have five images. Thus, the one sixth of loop in front of the corner reflector can act as a complete loop in free space.

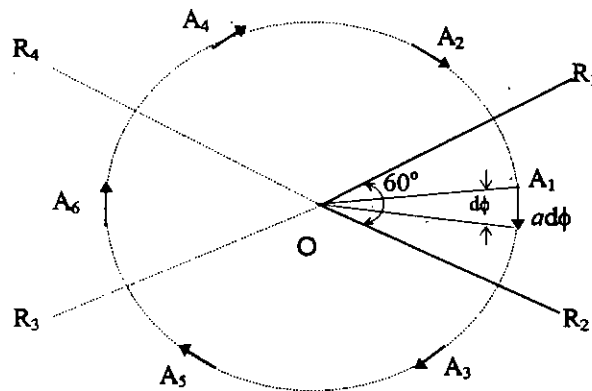


Fig. 2.3 Image produces by an infinitesimal dipole of one sixth of loop in front of a 60° corner reflector.

According to the image theory the effect of the image would be experienced only above the ground plane and beneath the ground plane which is known as the shadow region (i.e. no field will be available at this region). Thus the hexad of one sixth of loop referring to as H-Loop behaves as a complete loop with a field in front of the reflector and negligible field (ideally no radiation) behind the reflector.

2.3 ANTENNA PARAMETERS

Antenna parameters such as directivity, gain, radiation efficiency, and radiation pattern are determined analytically for the H-Loop antenna. General equations for determining the antenna parameters are described in the following subsections.

2.3.1 Directivity

The directivity of an antenna is an indicator of the relative directional properties of the antenna. The directivity (D) of an antenna is given by the ratio of the maximum radiation intensity ($U(\theta, \phi)_m$), in a given direction to the average radiation intensity (U_{av}) over all directions [8]. Thus the directivity in any direction (θ, ϕ) can be written as

$$D = \frac{U(\theta, \phi)_m}{U_{av}} \quad (2.8)$$

Again, the radiation intensity is defined as the power radiated per unit solid angle from the antenna. If P_r is the total radiated power then the average radiation intensity in all directions is given as

$$U_{av} = \frac{P_r}{4\pi} \quad (2.9)$$

The total radiated power P_r at a distant point from the antenna can be obtained from the average Poynting vector (S_r) which can be written as

$$S_r = \frac{1}{2} \Re e(\vec{E} \times \vec{H}^*) \quad (2.10)$$

The radial Poynting vector S_r can be determined from the E_ϕ and H_θ components of the electric and magnetic field respectively.

The total radiated power can then be obtained as

$$P_r = \int_{\phi=0}^{2\pi} \int_{\theta=0}^{\pi} S_r r^2 \sin\theta d\theta d\phi \quad (2.11)$$

In the case of H-Loop antenna radiated field is confined in front of the 60° corner reflector. Therefore, integration of eqn. 2.11 is to be performed for $0 \leq \theta \leq \pi$ and $0 \leq \phi \leq \pi/3$.

For the H-Loop antenna the eqn. 2.11 can be written as

$$P_r = \int_{\phi=0}^{\pi/3} \int_{\theta=0}^{\pi} S_r r^2 \sin\theta d\theta d\phi \quad (2.12)$$

The maximum radiation intensity for the H-Loop antenna, can be written as

$$\begin{aligned}
 P_r &= \int_{\phi=0}^{\pi/3} \int_{\theta=0}^{\pi} U_m \sin^2 \theta d\Omega \\
 &= \int_{\phi=0}^{\pi/3} \int_{\theta=0}^{\pi} U_m \sin^3 \theta d\theta d\phi \\
 &= \frac{4\pi}{9} U_m
 \end{aligned}$$

or,
$$U_m = \frac{9}{4\pi} P_r \quad (2.13)$$

Substituting, the value of P_r from eqn. 2.12 in eqn. 2.9 and eqn. 2.13, the value of average and maximum radiation intensity can be found respectively. The directivity of H-Loop antenna can then be found from eqn. 2.8.

2.3.2 Gain

The Gain (G) of the antenna can be determined from the directivity and the radiation efficiency of the antenna. G is given as [8]

$$G = \eta D \quad (2.14)$$

where η is the radiation efficiency. η is obtained as [8]

$$\eta = \frac{R_r}{R_r + R_{ohmic} + R_{ref}} \quad (2.15)$$

Where R_r = radiation resistance,

R_{ohmic} = ohmic resistance,

R_{ref} = reflector resistance.

2.3.3 Radiation pattern

There are three types of radiated field pattern obtained from the antenna. These are [8]:

- i) Radiated field pattern for the θ component of the electric field or $E_\theta(\theta, \phi)$ ($V\ m^{-1}$).
- ii) Radiated field pattern for the ϕ component of the electric field or $E_\phi(\theta, \phi)$ ($V\ m^{-1}$).
- iii) Field pattern for the phase of these fields as a function of the angles θ and ϕ or $\delta_\theta(\theta, \phi)$ and $\delta_\phi(\theta, \phi)$ (rad or deg).

A normalized field pattern can be obtained by dividing the field component by its maximum value. The normalized far field pattern of the electric field (E_ϕ), given as

$$E_\phi(\theta, \phi)_n = \frac{E_\phi(\theta, \phi)}{E_\phi(\theta, \phi)_{max}} \quad (2.16)$$

CHAPTER 3

MATHEMATICAL MODEL AND COMPARISON

- INTRODUCTION
- MATHEMATICAL MODEL OF H-LOOP ANTENNA
- H-LOOP ANTENNA PARAMETERS
- COMPARISON

3.0 INTRODUCTION

The mathematical model of the H-loop antenna has been developed by using image theory and the theory of pattern multiplication [8]. The radiated EM field due to the arc (one sixth of the loop) is to be calculated first and then applying image theory for determining the images of the arc. The effect of these images on the EM field of the original H-loop are then superimposed by a method similar to pattern multiplication.

Development of mathematical model is described in section 3.1. The mathematical formulation of important parameters of the H-Loop antenna are described in section 3.2. The antenna parameters of the H-Loop is compared with those of the existing Q-Loop antenna as well as the complete loop antenna. Comparison is given in section 3.3.

3.1 MATHEMATICAL MODEL OF H-LOOP ANTENNA

One sixth of loop in front of a 60° corner reflector produces five image loops of the original one. Thus the H-Loop antenna can be considered an array of coplanar three pair of dipoles shown in fig. 3.1.

Each pair of dipoles are parallel to each other carrying equal and out of phase current. It is assumed that the current through the arc is in the ϕ direction only, so the vector potential at any point in space will be ϕ directed only. The far field is computed from the vector potential of the one sixth of loop element and the vector potential of coplanar hexad dipoles.

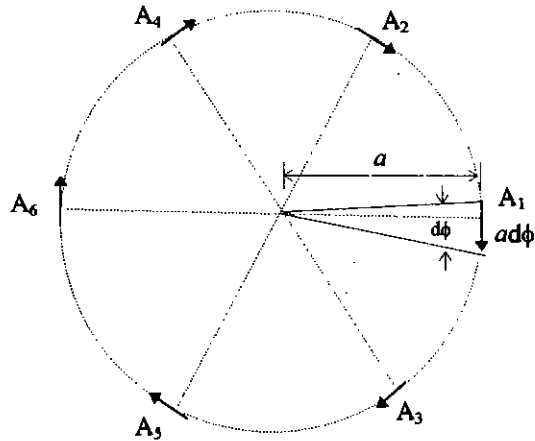


Fig. 3.1 Array of Coplanar three pairs of dipole.

The following assumptions have been made to determine the vector potential of coplanar hexad dipoles :

- * Distances between each dipole and the point of observation (P) shown in fig. 3.2 are parallel to the radial line ($op = r$).
- * A small loop is assumed (i.e. $a \ll \lambda$, and $a \ll r$, where a is the loop radius), thus during the distance calculation all terms which are less than a has been neglected whereas in phase calculation these terms have to be considered.

3.1.1 Distances between dipoles and observation points

Three pair of dipoles in the x-y plane of the rectangular coordinate system are shown in fig. 3.2. Each pair of dipoles are parallel to each other and opposite in phase.

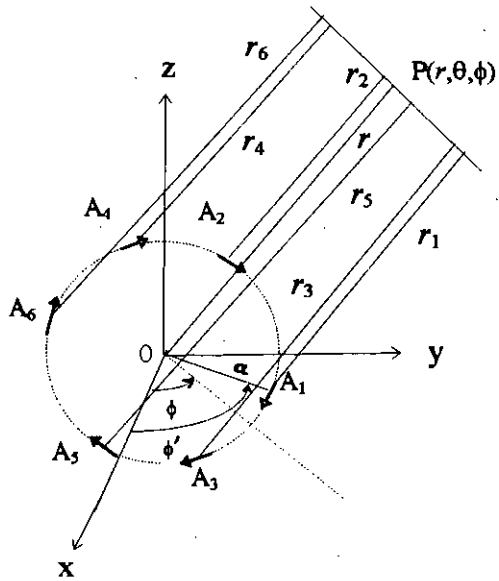


Fig. 3.2 Far field of three pair of dipoles, arbitrarily oriented w.r.t. the axes of co-ordinates.

A differential length $a d\phi$ of the arc at point A_1 is considered to compute the distance (r_1) between the point of observation $P(r, \theta, \phi)$ and the arc.

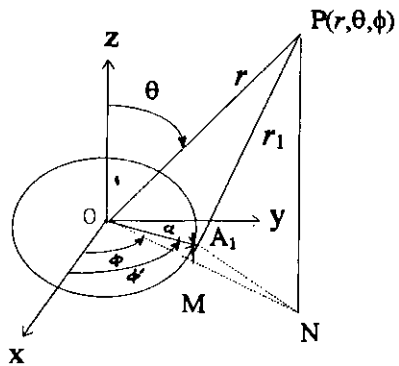


Fig. 3.3 Geometry of one sixth of loop for determining the vector potential of the H-Loop arc.

From fig. 3.3 the distance ($r_1 = PA$) can be written as

$$PA^2 = AN^2 + PN^2 \quad (3.1)$$

Again AN^2 can be written as

$$AN^2 = AM^2 + MN^2 \quad (3.2)$$

Where,

$$AM = a \sin(\phi' - \phi)$$

$$MN = [r \sin \theta - a \cos(\phi' - \phi)]$$

Substituting the expression for AM and MN in eqn. 3.2, the eqn. 3.2 can be written as

$$\begin{aligned} AN^2 &= a^2 \sin^2(\phi' - \phi) + [r \sin \theta - a \cos(\phi' - \phi)]^2 \\ &= a^2 + r^2 \sin^2 \theta - 2ra \sin \theta \cos(\phi' - \phi) \end{aligned} \quad (3.3)$$

The PN^2 is found as

$$PN^2 = r^2 \cos^2 \theta \quad (3.4)$$

Substituting eqn. 3.3 and eqn. 3.4 in eqn. 3.1 gives

$$\begin{aligned} r_1^2 = PA^2 &= a^2 + r^2 \sin^2 \theta - 2ra \sin \theta \cos(\phi' - \phi) + r^2 \cos^2 \theta \\ &= r^2 + a^2 - 2ra \sin \theta \cos(\phi' - \phi) \end{aligned} \quad (3.5)$$

For $r \gg a$, the eqn. 3.5 becomes as

$$r_1^2 = r^2 - 2ra \sin\theta \cos(\phi' - \phi)$$

$$\text{or, } r_1 = r \left[1 - \frac{2a}{r} \sin\theta \cos(\phi' - \phi) \right]^{1/2} \quad (3.6)$$

For distance consideration the first term of the eqn. 3.6 is taken and the r_1 becomes as

$$r_1 \cong r \quad (3.7)$$

For phase consideration the first two terms of the eqn. 3.6 are to be taken and the r_1 then becomes as

$$r_1 \cong r \left[1 - \frac{a}{r} \sin\theta \cos(\phi' - \phi) \right]$$

$$= r - a \sin\theta \cos(\phi' - \phi)$$

$$= r - a \sin\theta \cos(\phi - \phi') \quad (3.8)$$

Similarly, the distances between the observation points and the dipoles at A_2 , A_3 , A_4 , A_5 , and A_6 shown in fig. 3.2 can be computed as

$$r_2 = r - a \cos(\phi' - \phi + 60^\circ) \sin\theta$$

$$r_3 = r - a \cos(\phi' - \phi - 60^\circ) \sin\theta$$

$$r_4 = r + a \cos(\phi' - \phi - 60^\circ) \sin\theta$$

$$r_5 = r + a \cos(\phi' - \phi + 60^\circ) \sin\theta$$

$$r_6 = r + a \cos(\phi' - \phi) \sin\theta \quad (3.9)$$

3.1.2 Vector potential of coplanar hexad dipoles

It is well known that an arc can be considered as an array of infinitesimal dipole. To compute the vector potential of the one sixth of loop and coplanar hexad dipoles the differential length $a d\phi$ of the arc is considered at point A_1 shown in fig. 3.2. Hence the vector magnetic potential at point P due to this dipole of length $a d\phi$ containing the uniform current along the length at point A_1 can be written as [9]

$$\vec{A}_1 = ke^{j\beta a \cos(\phi' - \phi) \sin \theta} [\hat{x} \sin \phi' - \hat{y} \cos \phi'] \quad (3.10)$$

Where $k = \frac{\mu [I] a d\phi}{4\pi r_1}$

$[I] = I_0 e^{j(\omega t - \beta r)}$ = retarded current at the point of observation P with respect to the centre of the loop arc.

\hat{x} = the unit vector along the x direction of the rectangular co-ordinate system.

\hat{y} = the unit vector along the y direction of the rectangular co-ordinate system.

β = propagation constant = $(2\pi/\lambda)$.

Similarly, the vector magnetic potentials at point P due to the dipoles A_2 to A_6 can be written as

$$\begin{aligned} \vec{A}_2 &= ke^{j\beta a \cos(\phi' - \phi + 60^\circ) \sin \theta} [\hat{x} \sin(\phi' + 60^\circ) - \hat{y} \cos(\phi' + 60^\circ)] \\ \vec{A}_3 &= ke^{j\beta a \cos(\phi' - \phi - 60^\circ) \sin \theta} [\hat{x} \sin(\phi' - 60^\circ) - \hat{y} \cos(\phi' - 60^\circ)] \\ \vec{A}_4 &= -ke^{-j\beta a \cos(\phi' - \phi - 60^\circ) \sin \theta} [\hat{x} \sin(\phi' - 60^\circ) - \hat{y} \cos(\phi' - 60^\circ)] \\ \vec{A}_5 &= -ke^{-j\beta a \cos(\phi' - \phi + 60^\circ) \sin \theta} [\hat{x} \sin(\phi' + 60^\circ) - \hat{y} \cos(\phi' + 60^\circ)] \\ \vec{A}_6 &= -ke^{-j\beta a \cos(\phi' - \phi) \sin \theta} [\hat{x} \sin \phi' - \hat{y} \cos \phi'] \end{aligned} \quad (3.11)$$

The vector magnetic potential at point P due to the pair of parallel dipoles at points A₁ and A₆ can be written as

$$\begin{aligned}\vec{A}_{1+6} &= k \left[e^{j\beta a \cos(\phi' - \phi) \sin \theta} - e^{-j\beta a \cos(\phi' - \phi) \sin \theta} \right] [\hat{x} \sin \phi' - \hat{y} \cos \phi'] \\ &= 2jk \sin[\beta a \cos(\phi' - \phi) \sin \theta] [\hat{x} \sin \phi' - \hat{y} \cos \phi']\end{aligned}\quad (3.12)$$

For $\lambda \gg a$, and $\beta a \ll 1$, the eqn. 3.12 then becomes as

$$\vec{A}_{1+6} = 2jk\beta a \sin \theta \cos(\phi' - \phi) [\hat{x} \sin \phi' - \hat{y} \cos \phi'] \quad (3.13)$$

Similarly, vector magnetic potential for the pairs of dipoles at points A₂ and A₅, and A₃ and A₄ can be written as

$$\begin{aligned}\vec{A}_{2+5} &= 2jk\beta a \sin \theta \cos(\phi' - \phi + 60^\circ) [\hat{x} \sin(\phi' + 60^\circ) - \hat{y} \cos(\phi' + 60^\circ)] \\ \vec{A}_{3+4} &= 2jk\beta a \sin \theta \cos(\phi' - \phi - 60^\circ) [\hat{x} \sin(\phi' - 60^\circ) - \hat{y} \cos(\phi' - 60^\circ)]\end{aligned}\quad (3.14)$$

The resultant vector magnetic potential due to the three pair of dipoles at the far field point P(r, θ, ϕ), becomes as

$$\begin{aligned}\vec{A} &= \vec{A}_{1+6} + \vec{A}_{2+5} + \vec{A}_{3+4} \\ &= 2jk\beta a \sin \theta \left[\begin{aligned} &\left\{ \cos(\phi' - \phi) \sin \phi' + \cos(\phi' - \phi - 60^\circ) \sin(\phi' - 60^\circ) + \cos(\phi' - \phi + 60^\circ) \sin(\phi' + 60^\circ) \right\} \hat{x} \\ &\left[-\left\{ \cos(\phi' - \phi) \cos \phi' + \cos(\phi' - \phi - 60^\circ) \cos(\phi' - 60^\circ) + \cos(\phi' - \phi + 60^\circ) \cos(\phi' + 60^\circ) \right\} \hat{y} \right] \end{aligned} \right] \\ &= 3jk\beta a \sin \theta [\hat{x} \sin \phi - \hat{y} \cos \phi]\end{aligned}$$

$$= \hat{\phi} 3jk\beta a \sin\theta \quad (3.15)$$

where, $\hat{\phi}$ is the unit vector along ϕ direction.

It can be seen from eqn. 3.15 that, for any orientation of the three pair of parallel dipoles but opposite in phase, the resultant vector potential will be the $3j\beta a \sin\theta$ times of that of single dipole. The term $3j\beta a \sin\theta$ of eqn. 3.15 is known as the array factor.

3.1.3 Vector potential of the H-Loop element (or arc)

The vector potential (A_{arc}) at point $P(r,\theta,\phi)$ in free space due to the current in the one sixth of loop can be written as [9]

$$\vec{A}_{arc} = \frac{\mu[I]a}{4\pi r} \int_0^{\pi/3} e^{j\beta a \sin\theta \cos(\phi - \phi')} d\phi' \quad (3.16)$$

For $j\beta a \sin\theta = k'$ and $\phi - \phi' = \alpha$, the definite integral of the eqn. 3.16 then reduces to

$$\int_0^{\pi/3} e^{j\beta a \sin\theta \cos(\phi - \phi')} d\phi' = \int_{\phi - \pi/3}^{\phi} e^{k' \cos\alpha} d\alpha \quad (3.17)$$

The term $e^{k' \cos\alpha}$ can be expanded an infinite series as

$$e^{k' \cos\alpha} = 1 + k' \cos\alpha + \frac{k'^2}{2} \cos^2 \alpha + \dots \quad (3.18)$$

Substituting eqn. 3.18 in eqn. 3.17 and taking integration term by term gives

$$\int_{\phi-\pi/3}^{\phi} e^{k \cos \alpha} d\alpha = \int_{\phi-\pi/3}^{\phi} \left[1 + k \cos \alpha + \frac{k^2}{2} \cos^2 \alpha + \dots \right] d\alpha$$

$$= \frac{\pi}{3} + k \sin \left(\phi + \frac{\pi}{3} \right) + \text{terms containing higher power of } k \quad (3.19)$$

For a small loop $\beta a \ll 1$, and $|\sin \theta| \leq 1$, thus all the terms containing in eqn. 3.19 can be neglected. Thus the definite integral of eqn. 3.17 becomes as

$$\int_0^{\pi/3} e^{j\beta a \sin \theta \cos(\phi - \phi')} d\phi' \approx \frac{\pi}{3} \quad (3.20)$$

Substituting eqn. 3.20 in eqn. 3.16 gives the vector potential as

$$\vec{A}_{arc} = \frac{\mu [I] a}{4\pi r} \cdot \frac{\pi}{3} \vec{\phi} \quad (3.21)$$

It has already been mentioned in the previous section that the one sixth of loop (or 60° arc) can be considered as a collection of infinitesimal dipoles. Thus the same analysis can be extended for the original arc and its five similar images.

The resultant vector potential due to the three pairs of dipoles at the far field point $P(r, \theta, \phi)$, will be

$$\vec{A} = \hat{\phi} 3j\beta a \sin \theta \times \vec{A}_{arc} \quad (3.22)$$

3.1.4 Field computation

The radiated far electric field and magnetic field can be determined from the vector potential as [9]

$$\vec{E} \cong -j\omega\vec{A} \quad (3.23)$$

$$\vec{H} \cong -j\frac{\beta}{\mu}\vec{A} \quad (3.24)$$

It has already been mentioned in the previous chapter (section 2.1) that in the far field region of the H-Loop antenna, only ϕ component of the electric field and θ component of the magnetic field are found. Thus the far electric field and magnetic field produced by the arc alone can be obtained as

$$E_{\phi arc} = -j\omega A_{arc} \quad (3.25)$$

$$H_{\theta arc} = -j\frac{\beta}{\mu} A_{arc} \quad (3.26)$$

Substituting eqn. 3.21 in eqn. 3.25 and eqn. 3.26 gives

$$E_{\phi arc} = -j\omega \frac{\mu [I] a \pi}{4\pi r 3} \quad (3.27)$$

$$H_{\theta arc} = -j\beta \frac{[I] a \pi}{4\pi r 3} \quad (3.28)$$

The net electric field produced by the H-Loop in front of 60° corner reflector can be determined as

$$\begin{aligned}
E_{\phi} &= \text{Array factor} \times E_{\phi_{arc}} \\
&= \frac{\mu\omega[I]a}{4r} \beta a \sin\theta
\end{aligned} \tag{3.29}$$

Similarly, the net magnetic field produced by the H-Loop in front of the 60° corner reflector will be as

$$\begin{aligned}
H_{\theta} &= \text{Array factor} \times H_{\theta_{arc}} \\
&= \beta \frac{[I]a}{4r} \beta a \sin\theta
\end{aligned} \tag{3.30}$$

If the co-ordinate axes are chosen so that the loop is in the x-y plane and the reflectors OR₁ and OR₂ are parallel to plane of z, then the above field expressions are valid for azimuth angle ϕ of 0 to $\pi/3$ and the polar angle θ of 0 to π (i.e. in front of the reflector). Reflector is assumed as infinite ground plane. Thus neither magnetic nor electric field is present behind the reflector. The eqn. 3.29 and eqn. 3.30 can be written as

$$\begin{aligned}
E_{\phi} &= \frac{\mu\omega[I]a}{4r} \beta a \sin\theta && \text{for } 0 \leq \phi \leq \pi/3 \text{ and } 0 \leq \theta \leq \pi \\
&= 0 && \text{elsewhere}
\end{aligned} \tag{3.31}$$

$$\begin{aligned}
H_{\theta} &= \beta \frac{[I]a}{4r} \beta a \sin\theta && \text{for } 0 \leq \phi \leq \pi/3 \text{ and } 0 \leq \theta \leq \pi \\
&= 0 && \text{elsewhere}
\end{aligned} \tag{3.32}$$

The theoretical prediction of the planar radiation pattern according to eqns. 3.31 and 3.32 are shown in fig. 3.4.

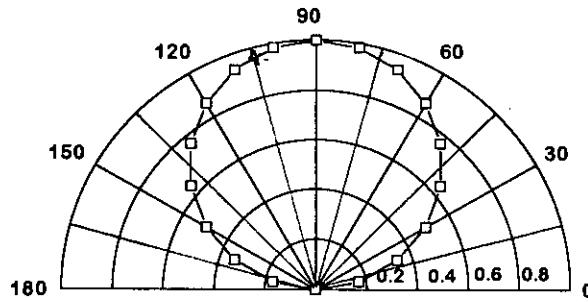


Fig. 3.4 (a) Planar radiation pattern (E_ϕ) of the H-Loop antenna at $\phi = 30^\circ$ plane with θ varying from 0 to 360° .

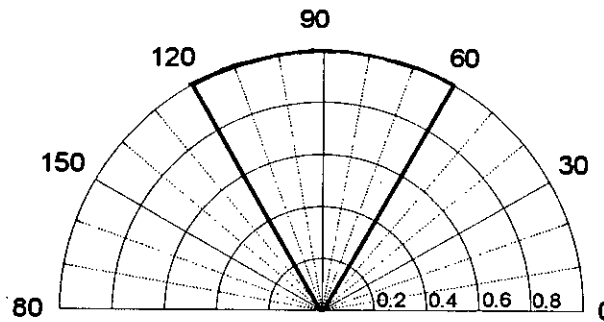


Fig. 3.4 (b) Planar radiation pattern (E_ϕ) of the H-Loop antenna at $\theta = 90^\circ$ plane with ϕ varying from 0 to 360° .

3.2 H-LOOP ANTENNA PARAMETERS

General expressions for finding the antenna parameters have already been given in previous chapter (refer to the section 2.3). The antenna parameters of the H-Loop have been derived from the general expression in the following subsections.

3.2.1 Directivity

The directivity is defined as the ratio of maximum radiation intensity to the average radiation intensity. The maximum and average radiation intensity can be obtained from the total power radiated by the H-Loop antenna. The total power radiated by the H-Loop antenna can be determined from eqn. 2.11 (refer to chapter-2), as

$$P_r = \int_{\phi=0}^{\pi/3} \int_{\theta=0}^{\pi} S_r r^2 \sin\theta d\theta d\phi \quad (3.33)$$

In the case of H-Loop, only the ϕ component of the electric field (E_ϕ) and the θ component of the magnetic field (H_θ) are found. Substituting the expression for E_ϕ (i.e. eqn. 3.31) and the expression for H_θ (i.e. eqn. 3.32) in eqn. 2.10 (refer to section 2.3.1) gives

$$S_r = \frac{15\beta^4 a^4 \pi I_o^2}{4r^2} \sin^2 \theta \quad (3.34)$$

Substituting eqn. 3.34 in eqn. 3.33 gives P_r as

$$P_r = \frac{5\pi^2 \beta^4 a^4 I_o^2}{3} \quad (3.35)$$

The maximum radiation intensity can be determined by substituting eqn. 3.35 in eqn. 2.13 (refer to chapter-2) as

$$U_m = \frac{9}{4\pi} P_r$$

$$= \frac{15\pi\beta^4 a^4 I_o^2}{4} \quad (3.36)$$

The average radiation intensity is computed as (by using eqn. 2.9 of chapter-2)

$$U_{av} = \frac{P_r}{4\pi}$$

$$= \frac{5\pi\beta^4 a^4 I_o^2}{12} \quad (3.37)$$

The directivity of H-Loop antenna is computed as

$$D_{H-loop} = \frac{U_m}{U_{av}} \quad (3.38)$$

$$= 9$$

3.2.2 Radiation resistance

Radiation resistance (R_r) of the H-Loop antenna can be determined as [8]

$$R_r = \frac{2P_r}{I_o^2} \quad (3.39)$$

where P_r is the total radiated power by the antenna and I_o is the maximum current flowing through the arc in time.

Substituting eqn. 3.35 in eqn. 3.39, yields

$$R_r = \frac{10}{3} \beta^4 (\pi a^2)^2 \quad (3.40)$$

$$= \frac{10}{3} \beta^4 A^2 \quad (3.41)$$

where A is the area of the loop. Eqn. 3.41 shows that the radiation resistance is independent of the size and shape of the loop wire.

3.2.3 Loop and Reflector resistance

Both the resistance of the loop and that of the reflector depends on the size and shape of the loop as well as material used for constructing the loop and reflector.

Ohmic or loss resistance of the antenna that carries uniform current is obtained as [10]

$$R_{ohmic} \approx \frac{l}{w} R_s \quad (3.42)$$

Where,

l = length of the antenna(arc) = $\pi a/3$

w = perimeter of the wire used for constructing the arc.

= $2\pi r_w$ for wire of circular cross-section.

= $4d$ for wire of square cross-section.

r_w = wire radius.

d = length of each side of the square wire.

R_s = surface resistance

R_s is determined as [10]

$$R_s = \sqrt{\frac{\omega\mu}{2\sigma}} \quad (3.43)$$

Where $\omega = 2\pi f$, f is the frequency, μ is the permeability and σ is the conductivity.

Substituting eqn. 3.43 in eqn. 3.42 gives

$$R_{ohmic} = \frac{a}{6r_w} \sqrt{\frac{\omega\mu}{2\sigma}} \quad (\text{for circular cross-section of the antenna wire}) \quad (3.44)$$

$$= \frac{\pi a}{12d} \sqrt{\frac{\omega\mu}{2\sigma}} \quad (\text{for square cross-section of the antenna wire}) \quad (3.45)$$

Similarly, the reflector resistance R_{ref} , can be determined as [6]

$$R_{ref} = \frac{a}{(w_r + t)} \sqrt{\frac{2\omega\mu}{\sigma}} \quad (3.46)$$

where w_r is the width of the reflector sheet and t is the thickness of the reflector sheet.

3.2.4 Inductance of the H-Loop

Self-inductance (L_H) of H-Loop antenna is the sum of internal inductance (L_{int-H}) and the external inductance (L_{ext-H}) of the antenna.

$$L_{H} = L_{int-H} + L_{ext-H} \quad (3.47)$$

Internal inductance L_{int-H} of a complete loop is obtained as [9]

$$L_{int} = \frac{\mu_0 l}{8\pi} \text{ henry} \quad (3.48)$$

Thus the L_{int-H} of the H-Loop antenna (i.e. one sixth of the loop) becomes as

$$L_{int} = \frac{\mu_0 a}{24} \text{ henry} \quad (3.49)$$

The eqn. 3.49 reveals that the internal inductance is independent of the cross-section of the loop wire.

External inductance L_{ext-H} of the H-Loop of circular cross-section is found as [9]

$$L_{ext-H} = a\mu \left[\ln\left(\frac{8a}{r}\right) - 2 \right] \text{ henry} \quad (3.50)$$

External inductance L_{ext-H} of the H-Loop of square cross-section is given as [11]

$$L_{ext-H} = \frac{\mu_0 a^2}{2} \int_0^{\pi/3} \frac{\cos\theta}{\sqrt{\left[\left(\frac{d}{2}\right)^2 + 2a\left(a - \frac{d}{2}\right)(1 - \cos\theta)\right]}} d\theta \quad (3.51)$$

3.2.5 Capacitance of the H-Loop

Two types of capacitance such as end capacitance and stray capacitance have to be considered. End capacitance is the capacitance between the flat end of the loop arc and the reflector, whereas the stray capacitance is the capacitance between the loop arc and the reflector. It is assumed that the stray capacitance is distributed along the loop.

For round wire total capacitance between the flat end of the one sixth of loop and the reflector (by neglecting the fringing capacitance), is obtained as

$$C_{end} = \epsilon_o \epsilon_r \frac{2\pi r_w^2}{t_n} \quad (3.52)$$

For wire of square cross section, total capacitance becomes as

$$C_{end} = \epsilon_o \epsilon_r \frac{2d^2}{t_n} \quad (3.53)$$

where r_w is the wire radius, d is the dimension of the square cross-section of the loop wire, ϵ_o is the absolute permittivity of the free space, ϵ_r is the relative permittivity of the insulating material (between the reflector and the loop arc) and t_n is the depth of this material which is the distance between the flat end of loop wire and the reflector.

The model of stray capacitance of the H-Loop antenna is shown in fig. 3.5. In calculating the stray capacitance fringing capacitance is neglected. Differential stray capacitance can be

obtained from the expression of capacitance of two parallel plate separated by a distance (d) (i.e. $\frac{\epsilon A}{d}$). Thus from the fig. 3.5 differential stray capacitance (dC) can be expressed as

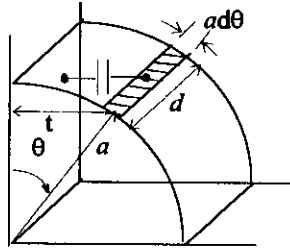


Fig. 3.5 Model of stray capacitance of the H-Loop antenna [6].

$$\begin{aligned}
 dC &= \epsilon_0 \frac{ad}{a \sin \theta} d\theta \\
 &= \epsilon_0 \frac{d}{\sin \theta} d\theta
 \end{aligned}
 \tag{3.54}$$

Where,

d = strip length

$ad\theta$ = the differential length of the arc

$dad\theta$ = strip area

$a \sin \theta$ = distance between the strip and the reflector

The total capacitance will be the twice of the capacitance between one half of the arc (θ varies from $\pi/6$ to $\pi/3$) and one side of the reflector. Thus the total stray capacitance for wire of square cross-section becomes as

$$\begin{aligned}
C_{stray} &= 2\varepsilon_0 d \int_{\pi/6}^{\pi/3} \frac{d\theta}{\sin\theta} \\
&= 2\varepsilon_0 d \ln \left[1 + \frac{2}{\sqrt{3}} \right]
\end{aligned} \tag{3.55}$$

Similarly, in the case of round wire, total stray capacitance can be obtained from eqn. 3.55, where the width d has to be replaced by the $r_w \sqrt{\pi}$. The total stray capacitance for wire of circular cross-section then becomes as

$$C_{stray} = 2\varepsilon_0 r_w \sqrt{\pi} \ln \left[1 + \frac{2}{\sqrt{3}} \right] \tag{3.56}$$

3.2.6 Gain

The gain of the H-Loop antenna (G_{H-Loop}) can be determined by using eqn. 2.14 as given in section 2.3.2 of chapter 2. Gain then becomes as

$$G_{H-loop} = \eta_{H-Loop} D_{H-loop} \tag{3.57}$$

where

D_{H-loop} = directivity of H-Loop antenna

η_{H-loop} = the radiation efficiency.

The radiation efficiency of H-Loop antenna can be determined by using eqn. 2.15 of section 2.3.2 of chapter 2, as

$$\eta_{H-Loop} = \frac{R_r}{R_r + R_{ohmic} + R_{ref}} \quad (3.58)$$

where

R_r = radiation resistance

R_{ohmic} = ohmic resistance

R_{ref} = reflector resistance.

Substituting eqns. 3.38 and 3.58 in eqn. 3.57 gives

$$G_{H-loop} = 9 \times \frac{R_r}{R_r + R_{ohmic} + R_{ref}} \quad (3.59)$$

Eqn. 3.59 depicts that G_{H-Loop} depends on the size and shape of the loop and frequency.

3.3 COMPARISON

The mathematical model, which is developed for the H-Loop antenna, has been compared with those of the existing Q-Loop antenna and the complete loop antenna. Comparison are given in the following subsections.

3.3.1 Comparison of field component with the Q-Loop antenna and complete loop antenna

The radiation pattern of the H-Loop antenna is similar to that of a Q-Loop antenna and that of Complete loop antenna. This can be shown from the field expression of these three types of loop antenna.

Expression of the radiated far fields for the H-Loop antenna are given in eqns. 3.31 and 3.32. The radiated far fields from a Q-Loop antenna are found as [6]

$$\begin{aligned}
 E_{\phi} &= \frac{\mu\omega[I]a}{4r} \beta a \sin\theta && \text{for } 0 \leq \phi \leq \pi/2 \text{ and } 0 \leq \theta \leq \pi \\
 &= 0 && \text{elsewhere}
 \end{aligned} \tag{3.60}$$

$$\begin{aligned}
 H_{\theta} &= \frac{\beta[I]a}{4r} \beta a \sin\theta && \text{for } 0 \leq \phi \leq \pi/2 \text{ and } 0 \leq \theta \leq \pi \\
 &= 0 && \text{elsewhere}
 \end{aligned} \tag{3.61}$$

On the other hand radiated far field from a complete loop antenna are given as [8]

$$\begin{aligned}
 E_{\phi} &= \frac{\mu\omega[I]a}{2r} J_1(\beta a \sin\theta) && \text{for } 0 \leq \phi \leq 2\pi \text{ and } 0 \leq \theta \leq \pi \\
 &= 0 && \text{elsewhere}
 \end{aligned} \tag{3.62}$$

$$\begin{aligned}
 H_{\theta} &= \frac{\beta[I]a}{2r} J_1(\beta a \sin\theta) && \text{for } 0 \leq \phi \leq 2\pi \text{ and } 0 \leq \theta \leq \pi \\
 &= 0 && \text{elsewhere}
 \end{aligned} \tag{3.63}$$

where, $[I]$ = Retarded current at the distant point w.r.t. the center of the loop.

$$= I_0 e^{j(\omega t - \beta r)}$$

I_0 = peak value of current in time (which is uniform along the loop arc).

$J_1(x)$ = Bessel function of first kind of argument x .

For small loop approximation, $J_1(\beta a \sin \theta) \approx (\beta a \sin \theta)/2$ then the eqn. 3.62 and eqn. 3.63 becomes as

$$E_\phi = \frac{\mu \omega [I] a}{4r} \beta a \sin \theta \quad \text{for } 0 \leq \phi \leq 2\pi \text{ and } 0 \leq \theta \leq \pi$$

$$= 0 \quad \text{elsewhere} \quad (3.64)$$

$$H_\theta = \frac{\beta [I] a}{4r} \beta a \sin \theta \quad \text{for } 0 \leq \phi \leq 2\pi \text{ and } 0 \leq \theta \leq \pi$$

$$= 0 \quad \text{elsewhere} \quad (3.65)$$

From eqns. 3.31, 3.32, 3.60, 3.61, 3.64, and 3.65 it is evident that though the radiation pattern of these three types of loops are identical, but the radiated field area is different from each other.

3.3.2 Antenna parameters

For comparison of the antenna parameters small loop is considered. Directivity and gain of these three loops are given in table - 1 and table - 2, respectively.

Table - 1 : Comparison of Directivity

Antenna	H-Loop	Q-Loop[6]	Complete Loop[8]
Directivity	9	6	3/2

Table - 1 shows that the directivity of H-Loop antenna is 1.5 times of Q-Loop antenna and 6 times of complete loop antenna. Thus it can be concluded that, H-Loop antenna is a highly directive antenna.

Table - 2 : Comparison of Gain

Antenna	H-Loop	Q-Loop[6]	Complete Loop[8]
Gain	$9 \times \frac{R_r}{R_r + R_{ohmic} + R_{ref}}$	$6 \times \frac{R_r}{R_r + R_{ohmic} + R_{ref}}$	$1.5 \times \frac{R_r}{R_r + R_{ohmic}}$

It is evident from table - 2 that for the same size and shape of the antenna and at the same frequency, the gain of H-Loop antenna is higher than that of the Q-loop and a complete loop antenna.

CHAPTER 4

DESIGN, CONSTRUCTION AND ANTENNA MEASUREMENT

- ❑ INTRODUCTION
- ❑ DESIGN CONSIDERATION OF FRACTIONAL LOOP
- ❑ CONSTRUCTION OF HEXAD OF A LOOP
- ❑ DESIGN CONSIDERATION OF THE REFLECTOR
- ❑ CONSTRUCTION OF THE REFLECTOR
- ❑ CONSTRUCTION OF THE H-LOOP ANTENNA
- ❑ FIELD MEASUREMENT
- ❑ COMPUTATION AND COMPARISON OF ANTENNA PARAMETERS

4.0 INTRODUCTION

Efficient radiation from the H-Loop in the desired frequency range depends on the size and shape of the one sixth of the loop. Thus various parameters which are to be considered in designing and constructing the one sixth of loop are described in section 4.1 and 4.2 respectively. Fractional loop is placed in front of the corner reflector to improve the directivity and to convert the one sixth of loop into a complete loop by image theory. Design and construction of the corner reflector are given in section 4.3 and 4.4 respectively. Section 4.5 gives the overall construction of the H-Loop antenna. Radiation pattern of the designed antenna is measured in the horizontal plane at various frequencies and at various radial distances. A description of the measurement set-up and procedure is given in section 4.6. Computation of antenna parameters of the designed antenna is given in section 4.7. The computed parameters is also compared with those of the Q-Loop and complete loop of the same size and shape of the designed H-Loop antenna. Comparison are also given in this section.

4.1 DESIGN CONSIDERATION OF FRACTIONAL LOOP

Antenna parameters such as the radiation efficiency and radiated power depends on the design parameters such as the loop radius, the size and the shape of the loop arc. An accurate selection of these design parameters are given in the following subsections.

4.1.1 Loop radius

A loop antenna of constant gain and maximum radiation efficiency in the frequency range of interest (30MHz to 1000MHz) is desirable. Gain and radiation efficiency are computed at

various loop radius. Gain and radiation efficiency at various frequencies as a function of loop radius are shown in figs. 4.1(a) and 4.1(b), respectively.

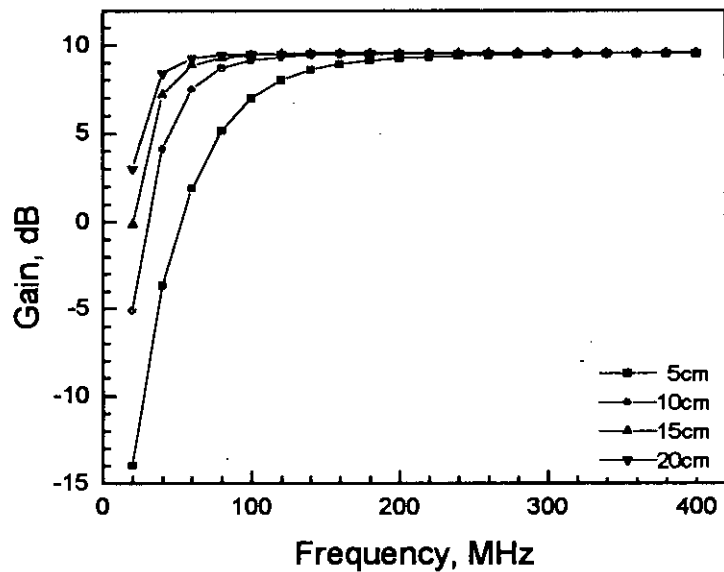


Fig. 4.1(a) Gain vs Frequency curve at various loop radius.

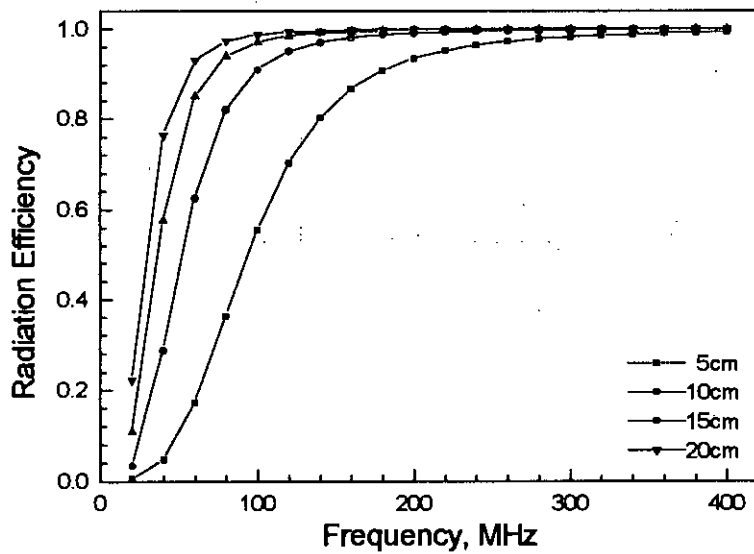


Fig. 4.1(b) Radiation Efficiency vs Frequency curve at various loop radius.

From fig. 4.1 it is evident that, the gain and radiation efficiency both increases with the increase of loop radius at frequencies below 100MHz. Above 100MHz, the gain and efficiency both are almost constant at all loop radius. However, maximum gain and radiation efficiency are found at frequency above 40MHz at a loop radius of 15cm. Thus, it is decided to select the loop radius of 15cm, because it can provide enough arc length for easy to bending at a 60° arc.

4.1.2 Shape and Dimension of the loop cross-section

Cross-sectional dimension of the loop wire is an important factor for the radiation efficiency at a fixed loop radius. In this work a wire of circular cross-section is chosen to construct the fractional loop. The radiation efficiency as a function of loop wire radius at various frequencies is shown in fig. 4.2.

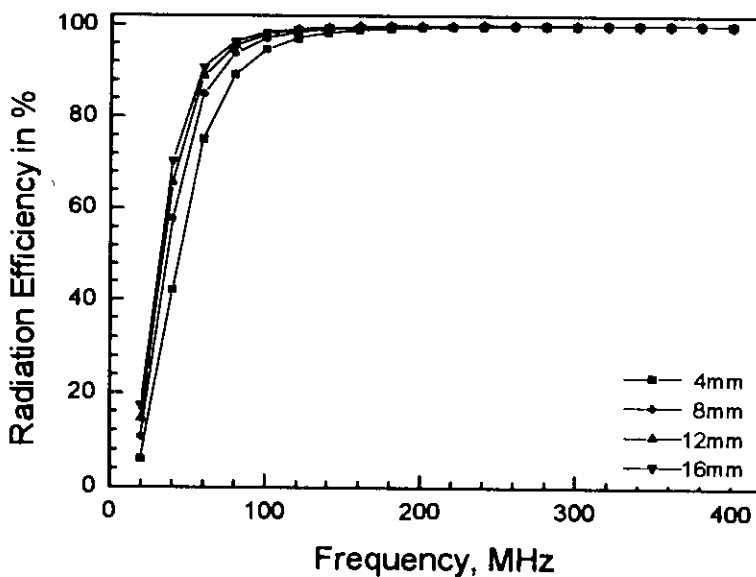


Fig. 4.2 Radiation efficiency vs Frequency curve at various wire radius.

Fig. 4.2 shows that the radiation efficiency increases with the increase of the wire radius at frequencies below 100MHz. However, a radiation efficiency of 85% is found at frequency above 40MHz at a wire radius of 8mm. Above 100MHz the radiation efficiency is almost constant at all wire radius. Thus it is decided to select the wire radius of 8mm, because it can provide enough space for mounting the connectors at the end of H-Loop, where it meets with the sides of the corner reflector.

4.2 CONSTRUCTION OF HEXAD OF A LOOP

Material of having good conductivity is always desirable during construction of the fractional loop for maximum radiation. Copper can be used for this purpose. But copper is costly and it is very difficult to machining. Thus, aluminum rod is used to construct the fractional loop, because aluminum is cheap and easy to machining.

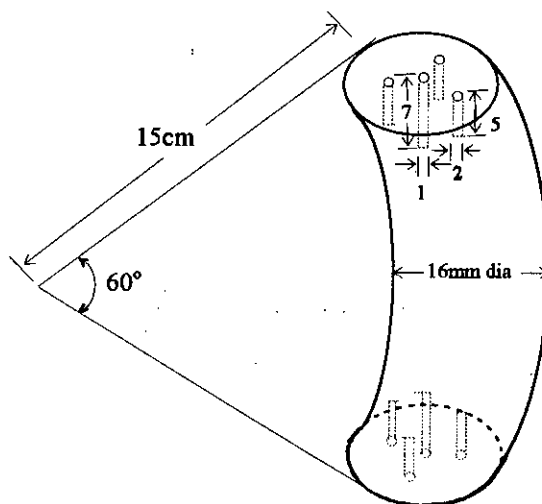


Fig. 4.3 (a) Sectional view of a hexad loop. Dimensions along the width and depth for the screw holes and for the centre stud of the BNC panel jack are shown (all the dimensions are in mm).

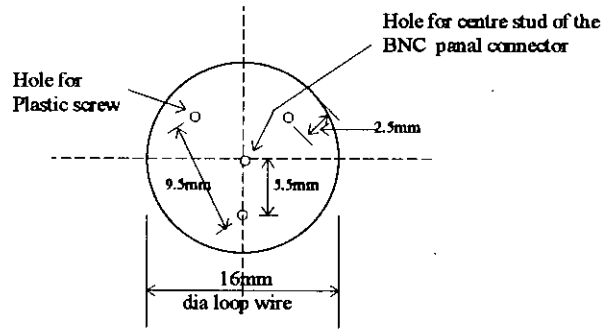


Fig.4.3 (b) *Dimensions and screw positions of the hexad loop.*

An aluminum rod of 16mm dia is bended at a 60° arc to construct a fractional loop of 15cm radius. The sectional view of the hexad loop is shown in fig. 4.3(a). Loop dimensions and screw positions for end connections at the flat ends are shown in fig. 4.3(b).

4.3 DESIGN CONSIDERATION OF THE REFLECTOR

A square corner reflector is used to improve the directional property as well as gain of the H-Loop antenna. The length of the reflector is to be large as compared to the antenna-to-corner spacing (i.e. the length of the loop radius), so that the reflector can be considered as an infinite ground plane to hold the image theory. The minimum length of each side of the square-corner reflector is considered to be the three times of the antenna-to-corner spacing (i.e. loop radius) [8]. Therefore, in this work each side of the reflector is assumed to be the four times of the loop radius (i.e. $4 \times 15 = 60\text{cm}$).

The region behind the sheet reflector would not be a full shadow region due to the sharp edge of the reflector. Thus the diffracted radiated field is found into the shadow region [12]. However, this diffracted radiation can be reduced by converting the sharp edges of the

reflectors into the rolled edges [13], which have a curvature of radius greater than $\lambda/4$. Thus in this work, the edges of the reflector are curved with a curvature radius of greater than 75cm to reduce the diffracted field at frequencies above 100MHz.

4.4 CONSTRUCTION OF THE REFLECTOR

Any metallic sheet of good conductivity can be used as a reflector. Copper or aluminum can be used. For the present work the flat aluminum sheet has been selected to construct the reflector because of its light weight and low cost. The main objective of the reflector is to achieve reflection from it, thus a sheet of any thickness can be used. However, the reflector should be strong enough so that it remains straight in any orientation. In this work an aluminum sheet of 2mm thickness is used in order to construct the reflector.

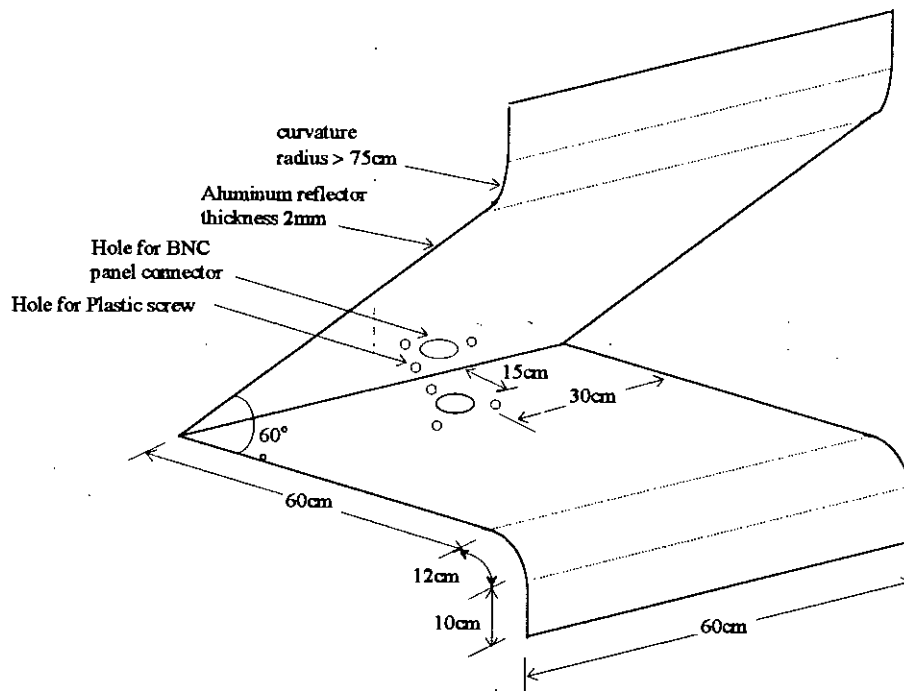


Fig.4.4 Design of a 60° corner reflector.

The reflector is constructed by bending a large Aluminum sheet at an angle of 60° . This reflector is shown in fig. 4.4. Each side of the square corner reflector is 60cm long (excluding the curved portion and flat extension). The length of the curved portion is considered to be 12cm and that of the flat extension is to be 10cm in order to reduce the edge diffraction as mentioned in the previous section.

4.5 CONSTRUCTION OF THE H-LOOP ANTENNA

The H-Loop antenna consists of 60° corner reflector and the one sixth of a loop as stated previously. Basically, reflector acts as a ground plane, thus it should be isolated from the one sixth of loop. Therefore, in constructing the H-Loop antenna, the one sixth of loop is mounted onto the inner side of the reflector. A thin rubber sheet with a hole at its center for passing the BNC panel jack is used as an isolation between the end of the loop and the side of the reflector. A groove is done at the flat end of the hexad loop to supply R.F. signal along the loop wire through BNC connector. Finally, the hexad loop is fixed onto the reflector by plastic screw. A diagram of the H-Loop antenna with end connections is shown in fig. 4.5. The photographs of front and top view of the H-Loop antenna are shown in figs. 4.6(a) and (b) respectively.

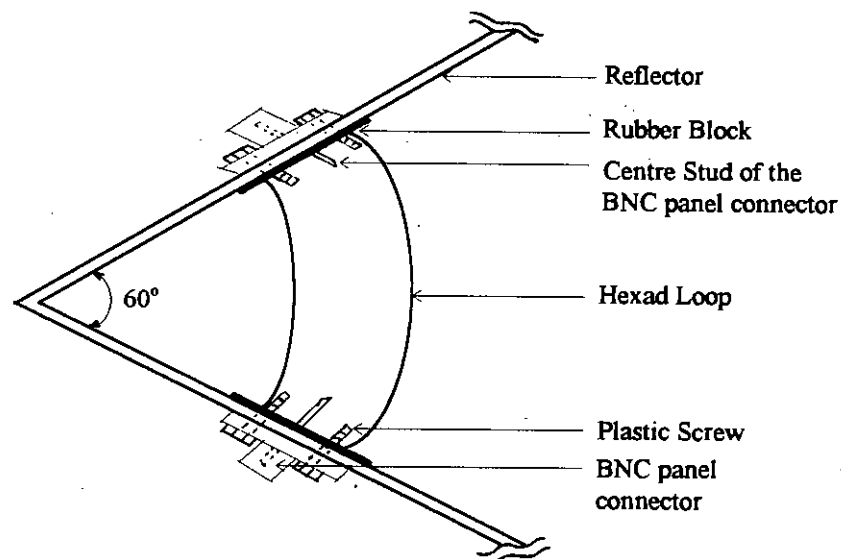


Fig. 4.5 Detailed diagram of H-Loop antenna.

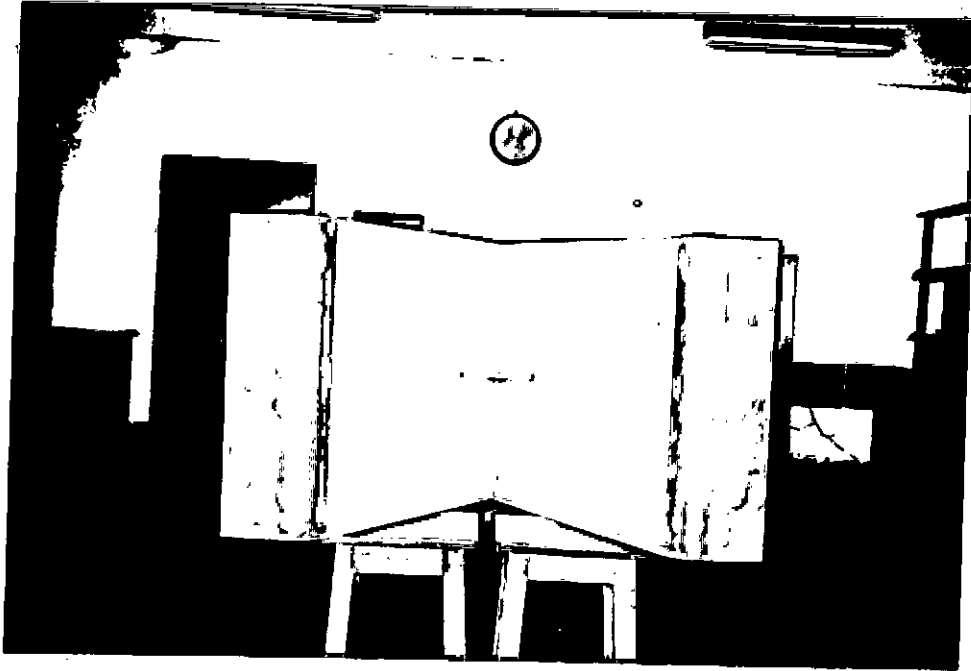


Fig.4.6 (a) *Photograph of front view of the H-Loop antenna.*

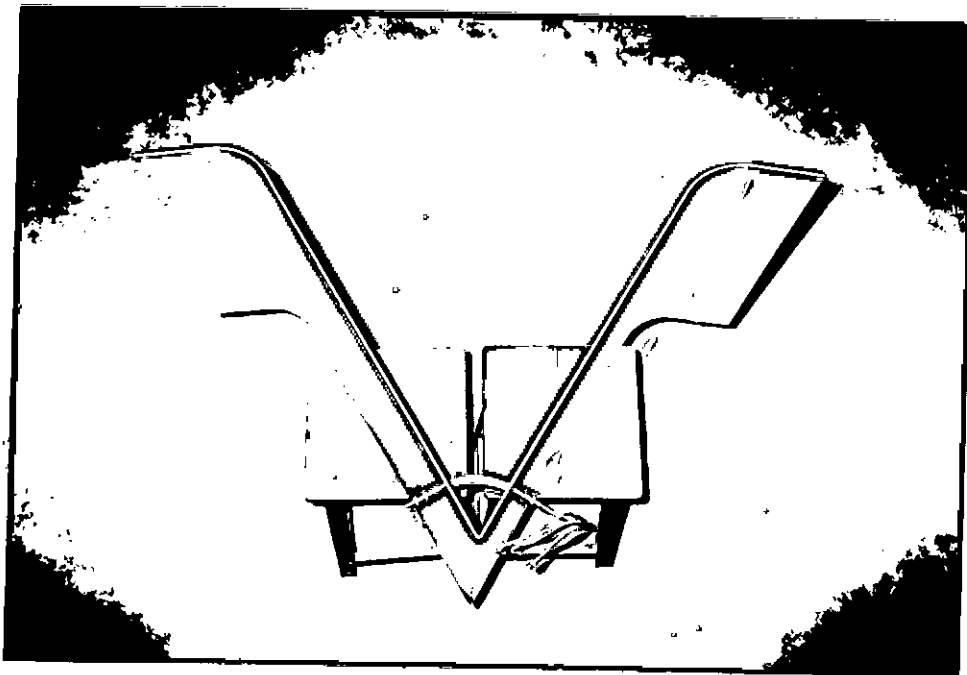


Fig.4.6 (b) *Photograph of top view of the H-Loop antenna.*

4.6 FIELD MEASUREMENT

For valid measurement of radiation patterns and other antenna parameters, measurement has to be carried out in a known EM environment. Two common test environment that are being employed for antenna measurement are as (i) open field and (ii) anechoic chamber.

Open area test site (OATS) is a convenient method for performing the radiation pattern measurement of an antenna. Standardised test site and the procedure for the measurement of radiated pattern in OATS is well described in the literature [14].

An anechoic chamber is an enclosure where metallic walls, ceiling and floor are lined by anechoic material that has a high absorption co-efficient. The anechoic material absorbs the incident EM energy on the wall, ceiling and floor from a source (i.e. antenna) within the enclosure and then provides a nearly reflection free enclosure. Anechoic chamber measurement is not suitable at low frequencies (below 200MHz). Because, generally anechoic material will be at least one quarter wavelength deep to absorb any appreciable amount of EM energy.

However, neither of the above mentioned standard test site was available during this research. Thus, the measurement was carried out in the laboratory environment which can cause measurement error. Only the radiation pattern of the developed H-Loop antenna is measured to compare the theoretical radiation pattern. Other antenna parameters such as gain, directivity and input impedance measurements were not possible due to the unavailability of the necessary instruments.

Throughout the measurement of radiation pattern, it is assumed that the H-Loop antenna is treated as a passive, linear and reciprocal devices. Therefore, this antenna can be used as both transmitting and the receiving mode during measurement of radiation pattern.

Test set-up, instruments and accessories required for the measurement of radiation pattern, feed arrangement, measurement procedure, test results and comparison are given in the following subsections.

4.6.1 Test set-up

It is assumed that the developed antenna holds reciprocity theorem. Thus the two H-Loop antenna of the same dimensions are constructed in order to experimentally observe the radiation pattern of the developed antenna. One is used as a transmitting antenna while the other is used as a receiving antenna. Schematic block diagram of the test set-up and a photograph of the test set-up is shown in fig. 4.7 and fig. 4.8 respectively.

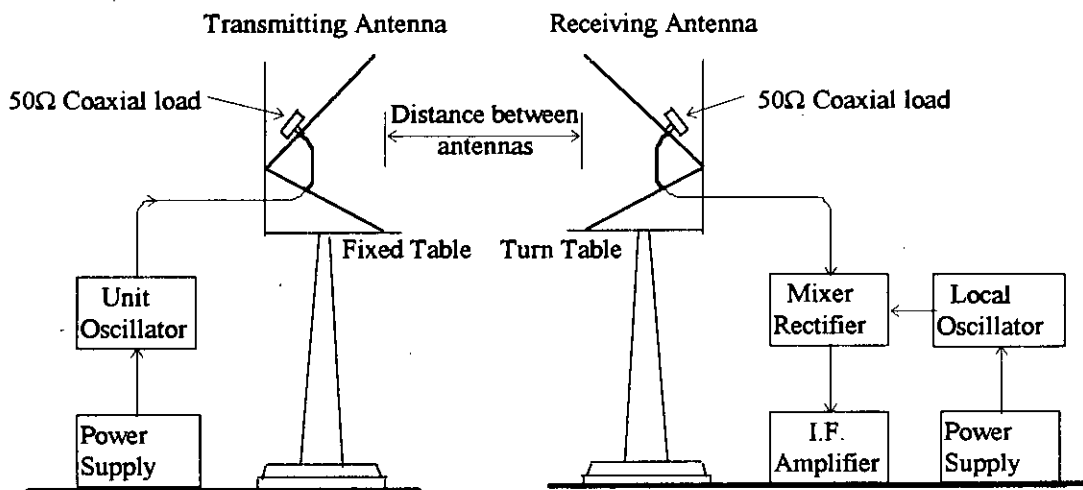


Fig. 4.7 Field Pattern Measurement set-up.

The receiving antenna is placed on a turn table to rotate it in the horizontal plane by varying the azimuth angle (ϕ) at polar angle $\theta = 90^\circ$. The angular position of this antenna is determined by an indicator and an angular scale fitted on the turn table.

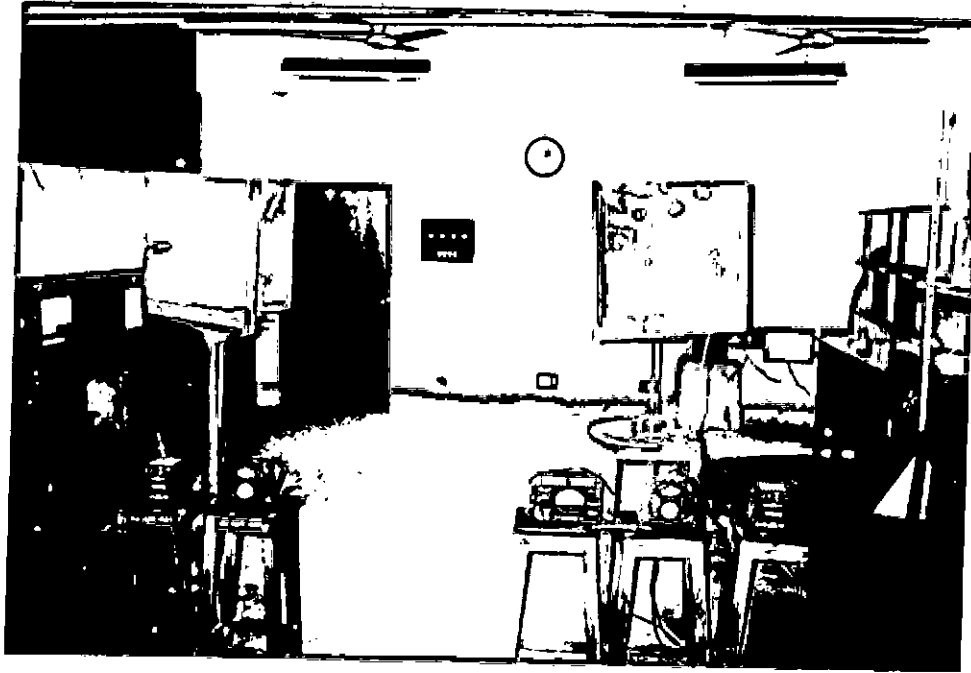


Fig. 4.8 *Photograph of field pattern measurement set-up.*

The input signal is fed into the one end of the transmitting antenna by a coaxial cable while the other side is terminated by a 50Ω coaxial load. On the other hand the one end of the receiving antenna is connected to the I.F. amplifier through a mixer rectifier for the measurement of EM field received by the antenna. The other end of the receiving antenna is also terminated by a 50Ω coaxial load.

4.6.2 Instrument and other Accessories for field measurement

Basic instruments for the field measurement include unit oscillator and I.F. amplifier. A unit oscillator is used to feed the R.F. signal into the transmitting antenna. At the receiving side another unit oscillator is used as a local oscillator. Accessories include 50Ω coaxial load, mixer rectifier, and BNC connectors.

Some relevant features of the unit oscillator, I.F. amplifier and mixer rectifier are given in the following subsections.

4.6.2.1 Unit Oscillator

Two General Radio Company Unit Oscillator (Type 1208-C) are used as a signal generator and local oscillator. The frequency range of this unit oscillator varies from 65 to 500MHz. Generator delivers a constant power of 240mW into a 50Ω load in the frequency range of 65MHz to 250MHz. Output power then decreases upto 80mW with the increase of frequency over the frequency range of 250MHz to 500MHz [15]. The output power level of 1208-C type unit oscillator is given in Appendix - A.

4.6.2.2 I.F. Amplifier and Mixer rectifier

The General Radio Company unit I.F. Amplifier (Type 1216-A) is a four-stage high-gain, intermediate-frequency amplifier operating at a frequency of 30MHz with a bandwidth of 0.7MHz [16]. A built-in meter which is calibrated in decibel (dB) indicates the relative signal level. A built-in precision resistance-type step attenuator determines the relative signal level beyond the range of the meter.

This type of amplifier is generally used in conjunction with a mixer rectifier and a unit oscillator to form a sensitive wide frequency-range, well-shielded VHF and UHF detector. In this work the General Radio Company Mixer Rectifier (Type 874-MR) is used along with the local oscillator to produce the difference signal (i.e. the difference between the signal received

by the antenna and the signal of the local oscillator) at the rectifier output. The block diagram of the mixer rectifier is shown in fig. 4.9.

A crystal diode of type 1N21-B, 250Ω series resistor, 40MHz low-pass filter and capacitor are used along with this mixer rectifier to make the 30MHz difference signal.

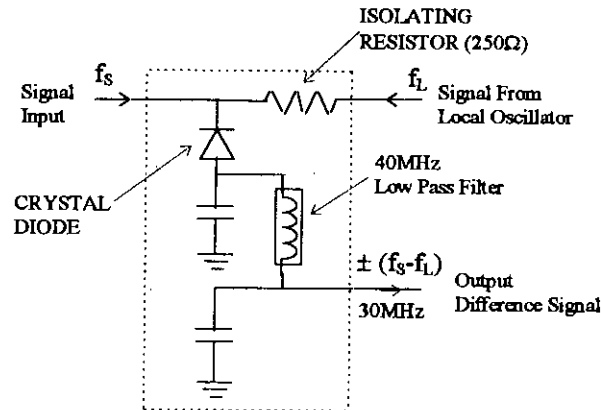


Fig.4.9 Block diagram of Type 874-MR Mixer Rectifier [16].

4.6.3 Feed arrangement

A photograph of the feeding arrangement with the load connections is shown in fig. 4.10. R.F. signal is to be fed into the loop wire from one end, while a 50Ω coaxial load is to be connected to the other end. Thus, 50Ω BNC panel connectors are fitted on the two sides of the reflector in such a way that the end terminal of the connectors becomes push-fit to the groove of the flat end of the loop.

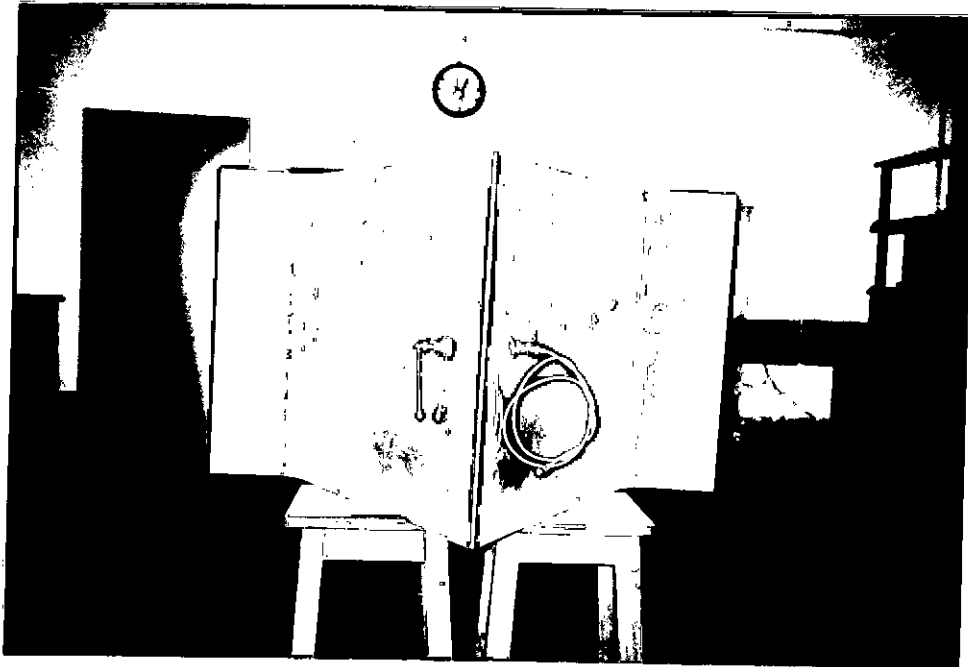


Fig.4.10 *Photograph of rear end of the H-Loop antenna.*

4.6.4 Measurement procedure

Field measurement is done at a radial distance of 1m and at frequency of 150MHz. The unit oscillator is adjusted to feed a 150MHz R.F. signal into the transmitting antenna. It has already been mentioned in the previous subsections that the operating frequency of the I.F amplifier is 30MHz. Thus the local oscillator at the receiving end is to be adjusted in such a way that a signal of frequency 30MHz (i.e. the difference between the local oscillator frequency and the received signal frequency) may be available at the output of mixer rectifier (refer to fig. 4.7). A 30MHz signal having maximum amplitude at the I.F. amplifier output indicates the accurate adjustment of the local oscillator. In order to obtain horizontal pattern, the receiving antenna is rotated in the horizontal plane (i.e. $\theta = 90^\circ$) where the azimuth angle (ϕ) varies from 0 to 180° .

The amplitude of the input signal of the I.F. amplifier is proportional to the amplitude of field received by the receiving antenna. This relationship has been derived in Appendix - B.

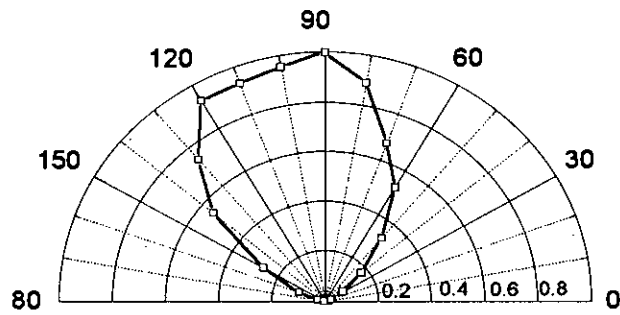
The receiving antenna is rotated to obtain the maximum field strength, which is found at $\phi = 90^\circ$, and $\theta = 90^\circ$. The position of maximum field strength is then considered as the reference position for the present task. The radiated EM field is recorded by rotating the receiving antenna in 10 degree steps in both the clockwise and counter-clockwise direction.

The measurement are repeated at frequencies 200MHz and 250MHz. Radiation pattern are also repeated at different radial distances ($r = 2\text{m}$ and $r = 3\text{m}$).

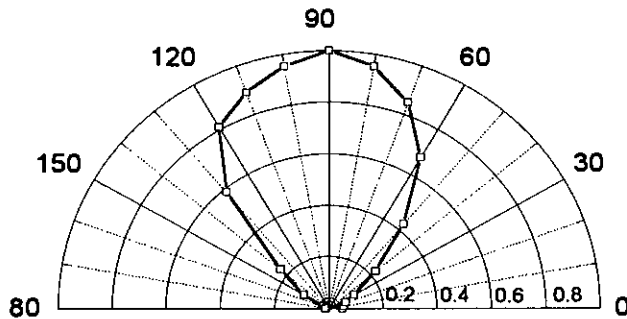
4.6.5 Test results and Comparison

It has already been mentioned in the previous chapter that the H-Loop antenna radiates in the azimuth angle (ϕ) varying from 0 to 60° in the horizontal plane (i.e. $\theta = 90^\circ$). In this work the reference position is considered at $\phi = 90^\circ$ and $\theta = 90^\circ$. Therefore, the presence of the radiated field is to be expected in between $\phi \geq 60^\circ$ and $\phi \leq 120^\circ$ in the same plane.

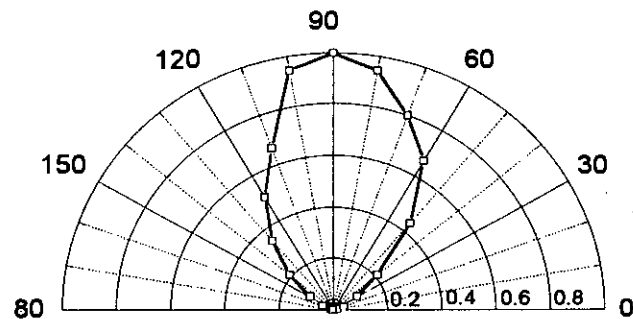
The measured field strength at different positions of the transmitting antenna are normalized by the maximum field strength which is obtained at the reference position. Polar plots of the measured radiated fields are shown in figs. 4.11 to 4.13.



(a)

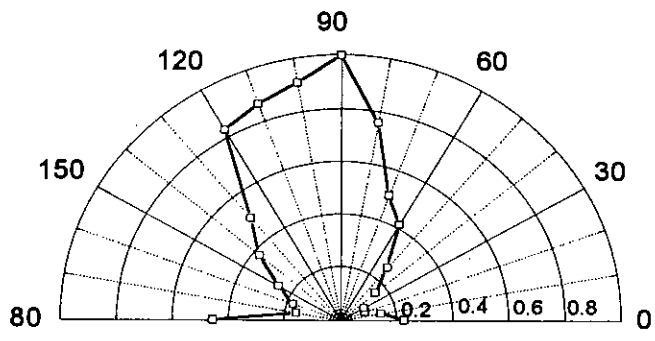


(b)

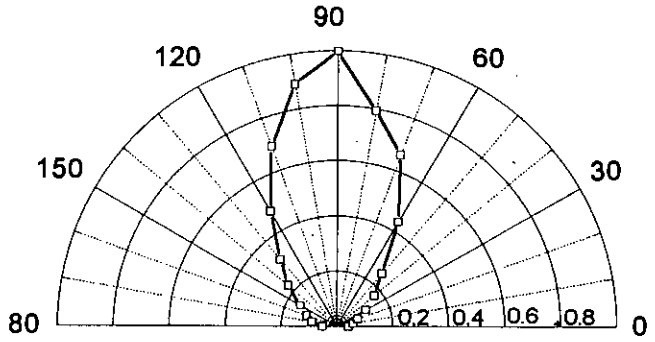


(c)

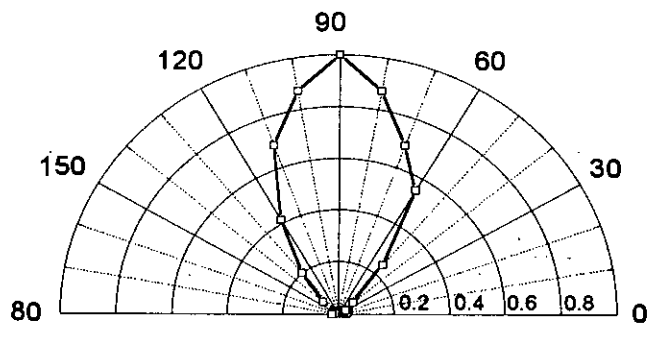
Fig. 4.11 Radiated field pattern at $\theta = 90^\circ$ and ϕ varying from 0 to 180° at a radial distance of 1m (a) 150MHz; (b) 200MHz; and (c) 250MHz.



(a)

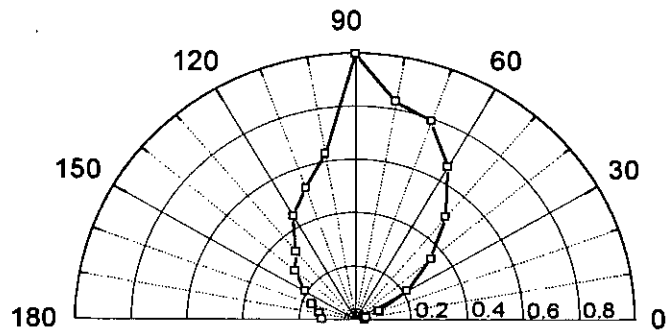


(b)

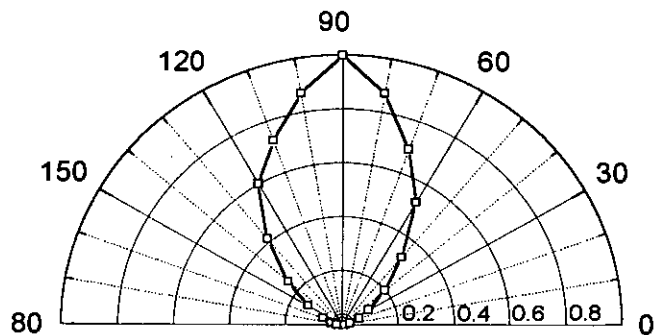


(c)

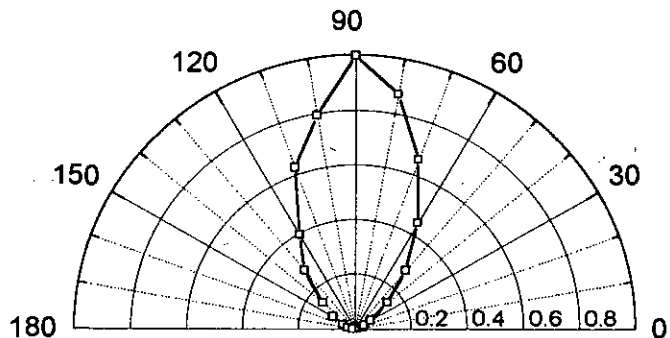
Fig. 4.12 Radiated field pattern at $\theta = 90^\circ$ and ϕ varying from 0 to 180° at a radial distance of $2m$ (a) $150MHz$; (b) $200MHz$; and (c) $250MHz$.



(a)



(b)



(c)

Fig. 4.13 Radiated field pattern at $\theta = 90^\circ$ and ϕ varying from 0 to 180° at a radial distance of 3m (a) 150MHz; (b) 200MHz; and (c) 250MHz.

To compare the measured field pattern with that of the theoretical field pattern the far electric field are computed by varying ϕ from 0 to 180° at $\theta = 90^\circ$. The computed normalized field pattern of the developed antenna is shown in the fig. 4.14. Figs. 4.11 to 4.14 shows that though the theoretical pattern and the measured pattern are identical but a weak field is found in the shadow region. In some cases field pattern is found to be distorted (see figs. 4.11 to 4.13).

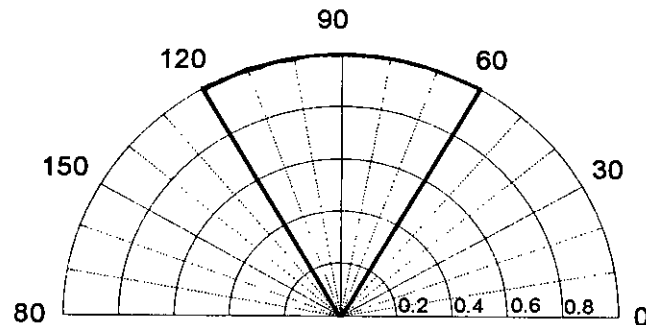


Fig. 4.14 *Theoretical radiated field pattern of the H-Loop antenna at $\theta = 90^\circ$ plane with ϕ varying from 0 to 180° .*

These may be due to the reflections from the metallic objects present in the room and associated cabling, radiation from the instruments, reception of other EM noise by both the receiving and transmitting antenna, the leakage current flowing through the reflector which also contributes to radiation. The distortion in the field pattern may also be due to the edge diffraction. Change in amplitude of the local oscillator during measurement can cause distortion in the radiation pattern.

4.7 COMPUTATION AND COMPARISON OF ANTENNA PARAMETERS

To find H-Loop antenna parameters, the following designed data are to be considered.

Wire radius (r_w) = 8mm

Mean loop radius (a) = 15cm

Reflector size = 60cm x 60cm x 2mm.

The above designed data are also to be considered to find the antenna parameters of the Q-Loop and the complete loop antenna.

4.7.1 Directivity

A comparison of the directivity of H-Loop antenna with those of the Q-Loop and the complete loop antenna are already given in the table - 1 of section 3.3.2 in chapter 3. Table shows that the directivity of H-Loop antenna is 1.5 times higher than that of Q-Loop and 6 times higher than that of complete loop antenna.

4.7.2 Gain

The gain of the loop antenna depends on the loop radius and the frequency of interest. Gain of the designed H-Loop antenna is computed at various frequencies by using eqn. 3.57 of chapter 3. A plot of the gain versus frequencies is shown in fig. 4.15.

Fig. 4.15 shows that the H-Loop antenna gain varies with frequency below 100MHz. Above 100MHz the gain of the H-Loop is constant. Thus this designed antenna can be considered as a frequency independent antenna above 100MHz.

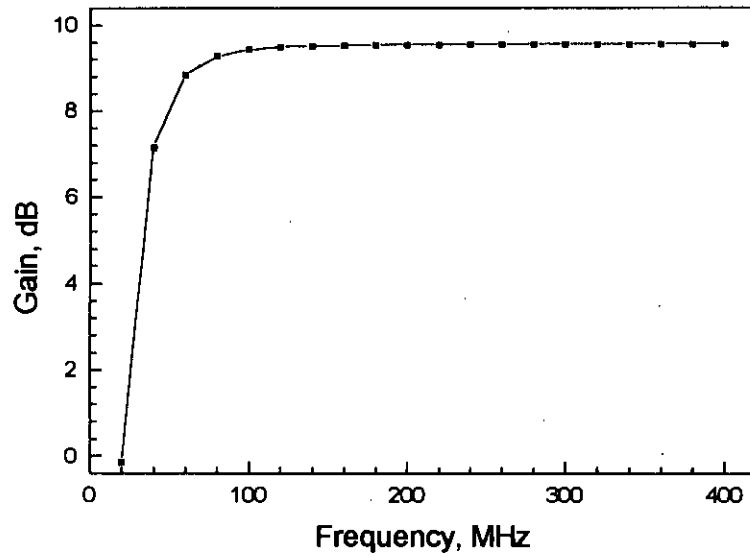


Fig. 4.15 Gain vs Frequency curve at a loop radius of 15cm.

The gain of the Q-Loop antenna and the complete loop antenna are also computed by using the formula given in the literature [6] and [8] respectively. A comparison of the gain among the three types of loop is shown in fig. 4.16. Fig. 4.16 shows that for the same input the H-Loop has higher gain than that of the Q-Loop as well as that of the complete loop.

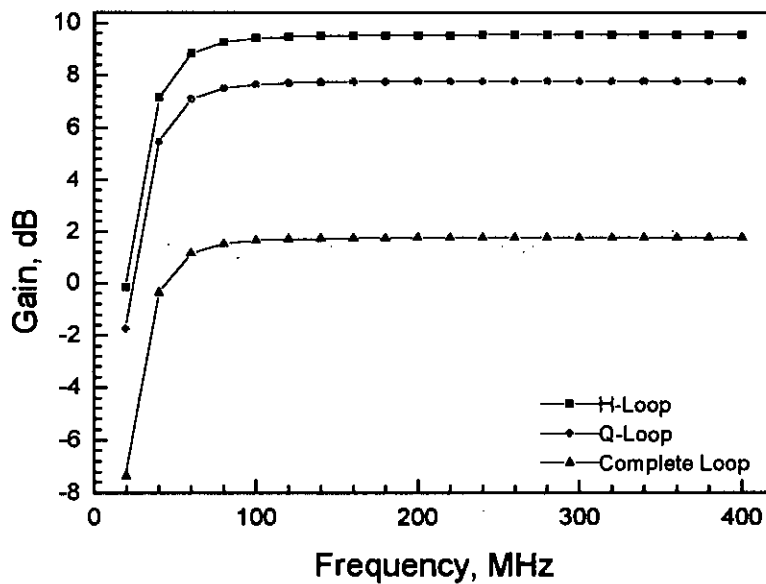


Fig. 4.16 Comparison of Gain vs Frequency curve of H-Loop, Q-Loop and Complete Loop antenna.

4.7.3 Radiation efficiency

The radiation efficiency of the designed H-Loop antenna is computed by using eqn. 3.58 of chapter 3. The radiation efficiency of the H-Loop antenna at various frequencies is shown in fig. 4.17.

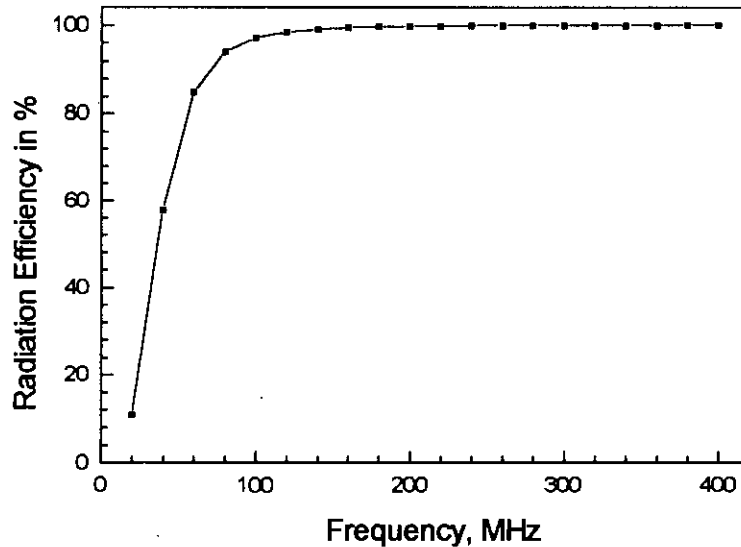


Fig. 4.17 Radiation efficiency vs Frequency curve at a given loop radius of 15cm.

The radiation efficiency of the complete loop antenna having the same loop radius as that of the H-Loop is also computed by using the formula given in the literature [8]. This comparison is shown in fig. 4.18. From the figure it is evident that the H-Loop has the same efficiency as that of the complete loop. This is due to the consideration of all five images in the case of H-Loop.

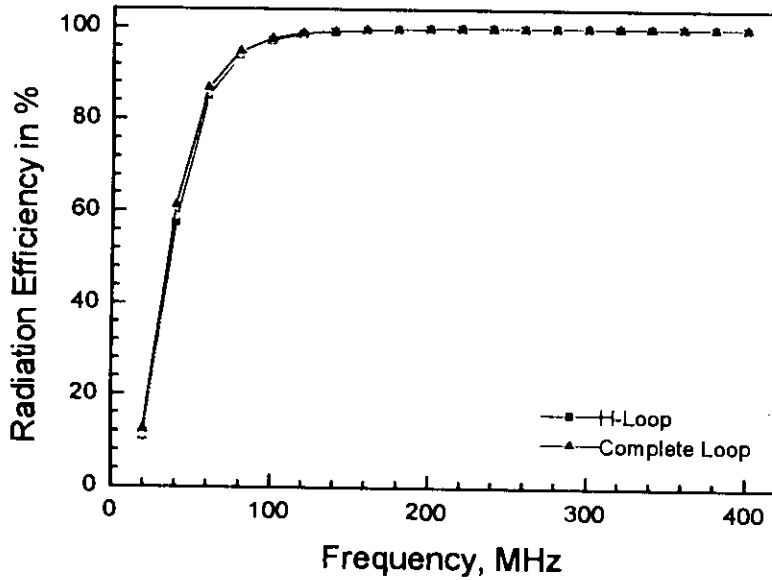


Fig. 4.18 Comparison of Radiation Efficiency vs Frequency curve of H-Loop and Complete Loop antenna.

4.7.4 Radiation resistance

Radiation resistance of the designed H-Loop antenna is computed by using eqn. 3.40 of chapter - 3. A plot of the radiation resistance (R_r) as a function of frequency is shown in fig. 4.19. The fig. 4.19 shows that the radiation resistance increases with the increase of frequency. This is desirable.

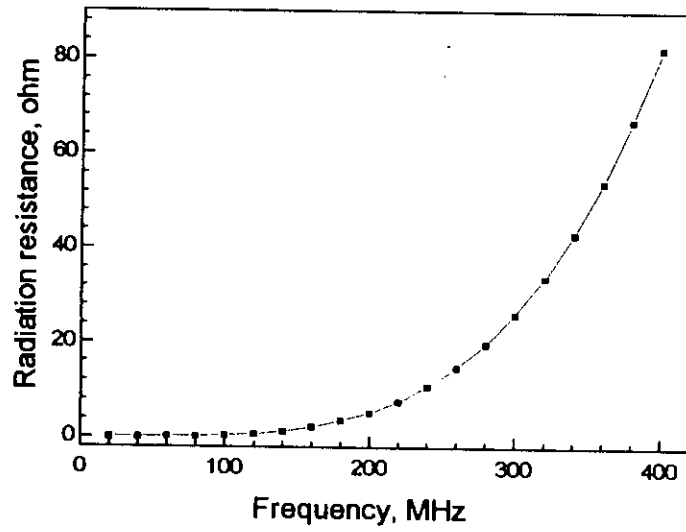


Fig. 4.19 *Radiation resistance vs Frequency curve at a given loop radius of 15cm.*

CHAPTER 5

CONCLUSION AND RECOMMENDATIONS FOR FUTURE WORK

- ❑ CONCLUSION
- ❑ RECOMMENDATIONS FOR FUTURE WORK

5.1 CONCLUSION

Development of an EMC antenna which could simulate standard EM waves, was the main objective of this research. This type of antenna can be used for the measurement of Shielding Effectiveness(SE) of conducting planar sheet. In this research work H-Loop antenna has been developed for producing low impedance magnetic field. Thus H-Loop can be employed to measure magnetic field SE of a planar sheet.

Some important features of EMC antennas along with the related theoretical background have been described in this thesis for better understanding of the salient features of the developed antenna. The radiation model, and antenna parameters of the H-Loop antenna have been derived analytically. It has been found that the radiation pattern of the H-Loop antenna is similar to that of the complete loop antenna. Complete loop antenna radiates over a solid angular surface of 360° , whereas the H-Loop antenna radiates over a solid angular surface of 60° , which is one-sixth of the surface of complete loop antenna and two-third of the surface of Q-loop antenna. This means that the H-Loop produces a low impedance field (i.e. magnetic field) in a quasi-shield test environment which is necessary for the measurement of magnetic field SE of a planar sheet material.

Antenna parameters such as directivity, gain and radiation efficiency of the H-Loop have been computed. These parameters are then compared with those of the Q-Loop antenna as well as those of the complete loop antenna. Comparison shows that (refer to table-1 of section 3.3.2 of chapter-3) the H-Loop has the directivity of 1.5 times of that of the Q-Loop and 6 times of that of the complete loop. The developed antenna gain is also higher than that of the Q-Loop and the complete loop (refer to fig. 4.16 of section 4.7.2 in chapter-4). It has also been found that the gain of the H-Loop becomes constant at frequency above 100MHz (refer to fig. 4.15 of section 4.7.2 of chapter 4). This indicates that the developed antenna can be treated as a frequency independent antenna above the frequency of 100MHz.

The typical EMC frequency ranges from 30MHz to 1000MHz. Thus at this frequency range of interest, two H-Loop antenna have been designed and then constructed. Size and shape of the one sixth of the loop has been selected in such a way which ensures the maximum radiated power, maximum gain and maximum radiation efficiency within the frequency range of interest. Reflector of the H-Loop produces images and also provides shielded environment. Thus a 60° corner reflector has been designed in such a way that the image theory holds as well as the edge diffraction effect can be minimized.

In this work it has been assumed that the developed antenna holds the reciprocity theorem. Thus, two H-Loop antenna have been used to measure the radiation pattern, where one acts as a transmitting antenna and the other acts as a receiving antenna. Measured radiation pattern has been found nearly identical to that of the computed pattern except at few cases. This may be due to the non-standard radiation pattern measurement environment.

Two H-Loop antenna (one acts as a transmitting antenna while the other acts as a receiving antenna) can be used to measure the low impedance magnetic field SE of a planar sheet like conductive material. H-Loop antenna can also be a promising type of magnetic field probe, which might be employed as near magnetic field characterisation of equipment for EMC testing.

5.2 RECOMMENDATIONS FOR FUTURE WORK

The following works are recommended to carry out in future.

In this work it has been assumed that the current distribution is uniform along the loop due to small loop approximation. Thus it is necessary to find the actual current distribution along the loop. The radiation pattern of the loop can then be determined from the current distribution. Determination of current distribution and radiation pattern could be a interesting research work in future. Current distribution in a half loop antenna has been described in the literature [17], which could be a guideline for this recommended research work.

In the present work the theoretical analysis of the H-Loop is based on the some assumptions and limitations as mentioned in section 3.1 of chapter 3. Thus in practical design consideration, the theoretical analysis of the H-Loop is needed further rigorous treatment by considering the limitation and assumption. Edge diffraction of the reflectors may also be considered during the rigorous analysis of the H-Loop.

Due to unavailability of the necessary instruments, it was not possible to measure the SE of the planar sheet during the research. Thus measurement of the magnetic field SE of different planar sheets could be carried out by using the developed H-Loop antenna.

Due to lack of the actual test environment (e.g. anechoic chamber, and OATS) and necessary instruments such as standard antenna and spectrum analyzer, it was not possible to measure the antenna parameters of the H-Loop. Measurement of the directivity, gain and input impedance could be carried out in future.

APPENDICES

APPENDIX A

OUTPUT POWER LEVEL OF A UNIT OSCILLATOR AT VARIOUS FREQUENCIES

The available power output from a Type 1208-C unit oscillator into a 50Ω coaxial load as a function of is shown in fig. A1.

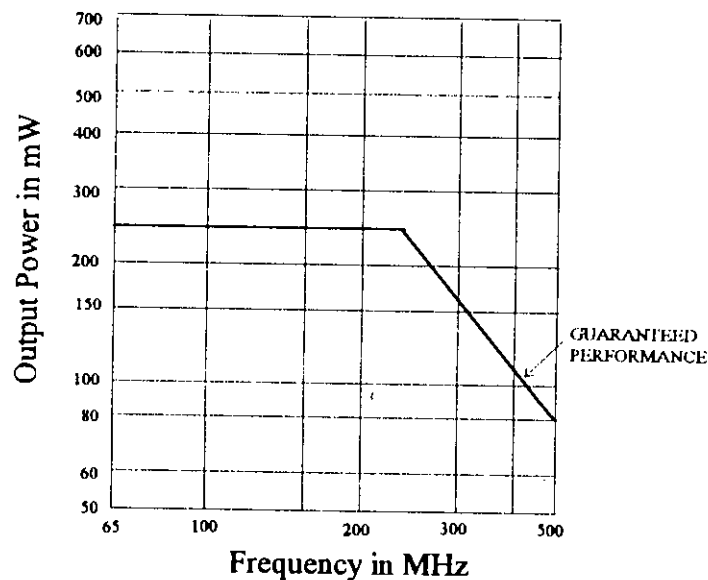


Fig. A1 Output power level of a typical type 1208-C unit oscillator into a 50Ω coaxial load [16].

The fig. A1 shows that, the unit oscillator (type 1208-C) delivers a constant power of 240mW from 65MHz to 250MHz frequency range. The output power then decreases above 250MHz. In the frequency range of 250MHz to 500MHz this power reduces upto 80mW.

Therefore, for maintaining constant power level, the unit oscillator (type 1208-C) has to be operated within the frequency range of 65 to 250MHz.

APPENDIX B

RELATION BETWEEN THE AMPLITUDE OF THE RADIATED FIELD AND THE AMPLITUDE OF THE INPUT SIGNAL OF THE I.F. AMPLIFIER

The detailed block diagram of the receiving section of field pattern measurement set-up is shown in fig. B1. The received signal (f_s), is fed into the mixer rectifier. A signal (f_L) from the local oscillator is also fed into the mixer rectifier.

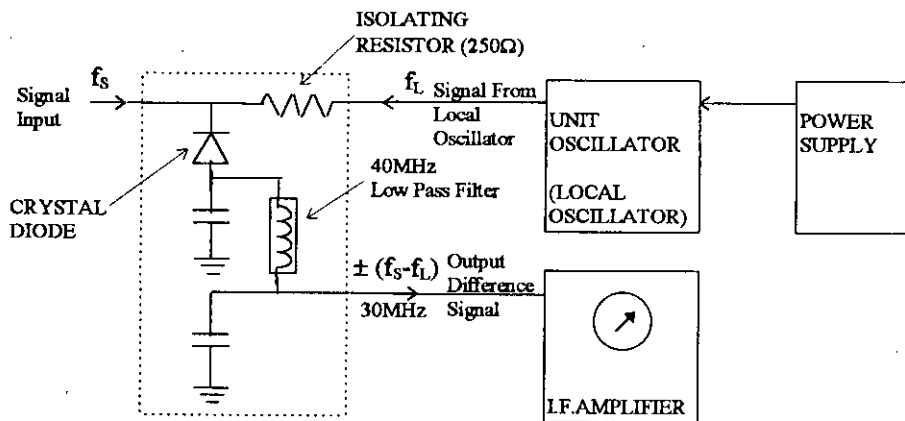


Fig. B1 Block diagram of the receiving section of field pattern measurement set-up.

The local oscillator is adjusted in such a way that the mixer rectifier produce an output signal (i.e. $\pm(f_s - f_L)$) of 30MHz. This difference signal is then fed into the I.F. amplifier. As mentioned in the chapter - 4, the I.F. amplifier responses at 30MHz frequency. The amplitude of the input signal of the I.F. amplifier is proportional to the field received by the receiving antenna (i.e. the field radiated by the transmitting antenna).

This relationship can be described mathematically as follows:

Let,

E_O = instantaneous value of the output difference signal (i.e. input signal of the I.F. amplifier) from the mixer rectifier

E_S = instantaneous value of the signal received by the receiving antenna

E_{Sm} = maximum value of E_S

E_{SO} = r.m.s. value of E_S

E_L = instantaneous value of the signal from local oscillator

E_{Lm} = maximum value of E_L

E_{LO} = r.m.s. value of E_L

According to the characteristics of mixer rectifier, E_O can be written as

$$\begin{aligned}
 E_O &\propto (E_S + E_L)^2 \\
 &\propto (E_{Sm} \sin \omega_S t + E_{Lm} \sin \omega_L t)^2 \\
 &\propto (E_{Sm}^2 \sin^2 \omega_S t + E_{Lm}^2 \sin^2 \omega_L t + 2E_{Sm}E_{Lm} \sin \omega_S t \sin \omega_L t) \\
 &\propto [E_{Sm}^2 \sin^2 \omega_S t + E_{Lm}^2 \sin^2 \omega_L t + E_{Sm}E_{Lm} \{ \cos(\omega_{Sm} - \omega_{Lm})t - \cos(\omega_{Sm} + \omega_{Lm})t \}] \quad (B.1)
 \end{aligned}$$

For the output difference signal, only the third term of the eqn. B.1 has been considered.

Thus eqn. B.1 becomes as

$$\begin{aligned}
 E_O &\propto E_{Sm}E_{Lm} \cos(\omega_{Sm} - \omega_{Lm})t \\
 &= 2K \cdot \frac{E_{Sm}}{\sqrt{2}} \cdot \frac{E_{Lm}}{\sqrt{2}} \\
 &= 2KE_{SO}E_{LO} \quad (B.2)
 \end{aligned}$$

where K is a constant.

It has been stated [15] that the output power level of the local oscillator is constant in the frequency range of 65MHz to 250MHz. Thus for this frequency range, the eqn. B.2 can be written as

$$E_o \propto E_{so} \tag{B.3}$$

The eqn. B.3 reveals that, the amplitude of the I.F. amplifier output is proportional to the amplitude of the received signal.

REFERENCES

- [1] S.A.Schelkunoff, *Electromagnetic Waves*, New York : Van Nostrand, 1943, pp.303-315.
- [2] Henry, W.Ott, *Noise Reduction Techniques in Electronic Systems*, 2nd ed., John Wiley and Sons, Singapore.
- [3] The Chase guide to EMC emission measurement, *Poster published by Chase ADVANTEST*, 1992.
- [4] MIL-STD-285, "Attenuation measurement for enclosures, electromagnetic shielding, for electronic test purposes, method of," August 1956.
- [5] L.C. Oberholtzer, " A Treatise of the NEW ASTM EMI Shielding Standard," *ITEM*, pp. 174-178, 1984.
- [6] H.Rahman, " Development of EMC Antenna and their Application in On-line SE Measurement of Conducting Composite Plastic Materials", *Ph.D. Thesis*, School of Electronic Engineering, Dublin City University, Ireland, March 1994.
- [7] P.A. Chatterton and M.A. Houlden, *EMC Electromagnetic Theory to Practical Design*, John Wiley and Sons Inc., Chichester, 1992.
- [8] J.D. Krauss, *Antennas*, 2nd ed., McGraw-Hill Inc., Singapore, 1988.
- [9] S. Ramo, J.R. Whinnery and T. Van Duzzor, *Fields and Waves in Communication Electronics*, NY: John Wiley and Sons Inc., 2nd ed., 1984.
- [10] W.L. Stutzman and G.A. Thiele, *Antenna Theory and Design*, NY: John Wiley and Sons Inc., pp. 394, 1981.
- [11] Plonsey, R. and Collin, R.F., *Principles and Applications of Electromagnetic Fields*, NY: McGraw-Hill, 1961.
- [12] J.D. Krauss, *Radio Astronomy*, 2nd ed., Cygnus-Quasar, pp. 642-646, 1986.
- [13] W.D. Burnside *et. al.*, " Curved edge modification of compact range reflectors ", *IEEE Trans., Antennas and Propagation*, AP-35, pp. 176-182, Feb. 1987.
- [14] " Recommended methods of measurement of radiated and conducted interference from receivers for amplitude-modulation, frequency modulation, and television broadcast transmission", Int. Electro-Tech. Commission Pub. 106, 1974.

- [15] " Operating Instructional Manual of Type 1208-C Unit Oscillator", General Radio Company, West Concord, Massachusetts, USA, 1967.
- [16] " Operating Instructional Manual of Type 1216-A Unit I.F. Amplifier", General Radio Company, West Concord, Massachusetts, USA, 1963.
- [17] Zhou, G. and Smith, G. S., " An accurate theoretical model for thin-wire circular half-loop antenna", *IEEE Trans., Antennas and Propagation*, vol. 39, no. 8, pp. 1167-1177, Aug. 1991.

